Characterization of the Alkali Metal Oxalates ($MC_2O_4^-$) and their formation by CO_2 reduction via the Alkali Metal Carbonites (MCO_2^-)

Joakim S. Jestilä[1], Joanna K. Denton[2], Evan H. Perez[2], Thien Khuu[2], Edoardo Apra[3], Sotiris S. Xantheas[4,5], Mark A. Johnson[2] and Einar Uggerud[1]

[1] Department of Chemistry and Hylleraas Centre for Quantum Molecular Sciences, University of Oslo, PO Box 1033, Blindern, Oslo N-0135, Norway

[2] Sterling Chemistry Laboratory, Yale University, New Haven, Connecticut 06520, United States

[3] Environmental Molecular Sciences Laboratory, Pacific Northwest National Laboratory, P.O. Box 999, Richland, Washington 99352, United States

[4] Advanced Computing, Mathematics and Data Division, Pacific Northwest National Laboratory, 902 Battelle Boulevard, P.O. Box 999, MS K1-83, Richland, Washington United States

[5] Department of Chemistry, University of Washington, Seattle, Washington 98195, United States

Supporting information

Table of Contents

SI-A. Mass spectra of oxalic acid and metal chlorides and hydroxides

Mass spectra of oxalic acid and metal chloride/hydroxide dissolved in water-methanol solutions are presented in Figure S1 –Figure ***S5***, whence the following are induced.

- Addition of triethylamine (TEA) or use of the metal hydroxide (MOH) as the source for the metal cations generally leads to improved metal oxalate peak intensities relative to the deprotonated oxalate peak.
- The base peak is most often due to the deprotonated acid, hydrogen oxalate ($HC_2O_4^-$), followed by the metal oxalate ($MC_2O_4^-$) or the metal hydrogen oxalate dimer ($M^+(HC_2O_4^-)_2$) peaks in terms of decreasing intensity. The dimer peak intensities relative to the base and monomer peaks tend to increase with metal size.
- Use of metal hydroxides generally yield "cleaner" mass spectra with fewer and higher peaks compared to the metal chlorides.
- TEA (10%) effectively removes the $RbCl_2^-$ peak from the mass spectrum of oxalic acid and RbCl.

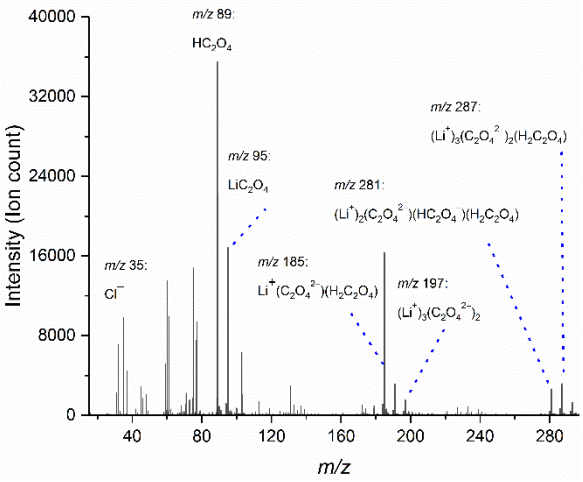

Figure S1. MS of 4mM Oxalic acid and 6 mM LiCl in 50/50 water/methanol with 1 % triethylamine (TEA).

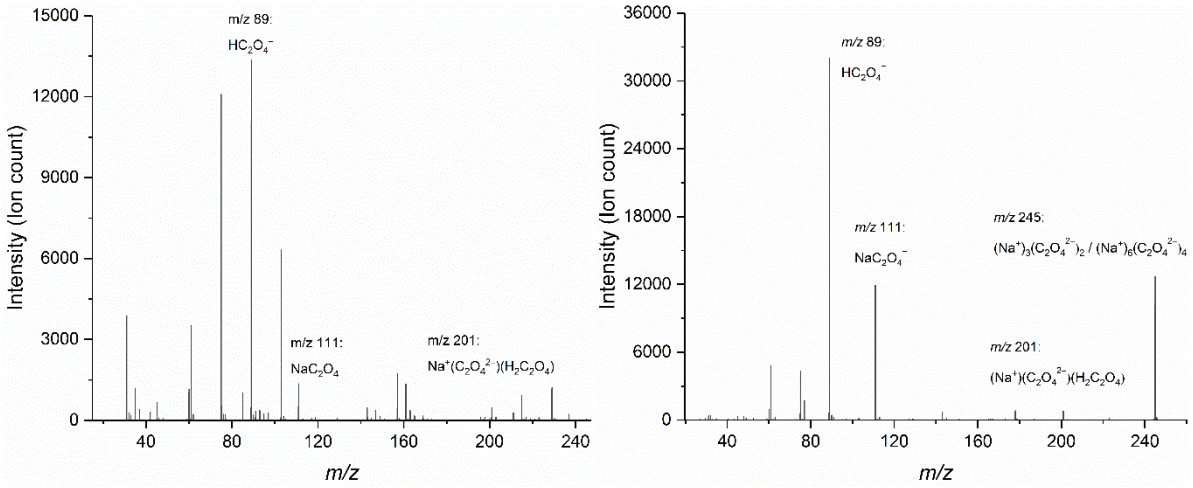

Figure S2. MS of 3.3 mM oxalic acid and 1.3 mM NaCl in 40/60 water/methanol (*left*), and of 2.9 mM oxalic acid and 5.3 mM NaOH in 50/50 water/methanol (*right*).

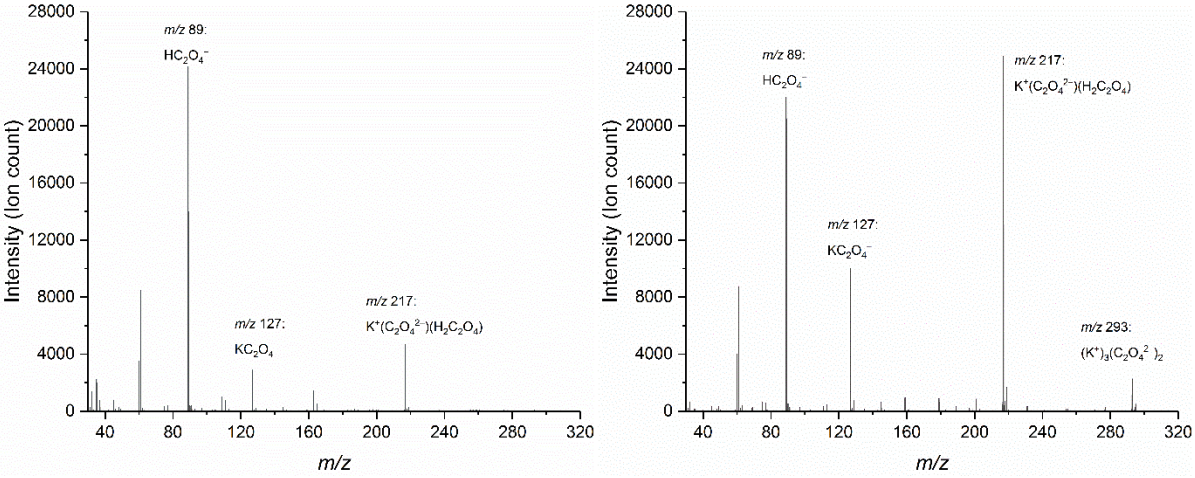

Figure S3. MS of 3.0 mM oxalic acid and 3.0 mM KCl in 50/50 water/methanol (*left*), and of 3.0 mM oxalic acid and 5.0 mM KOH in 50/50 water/methanol (*right*).

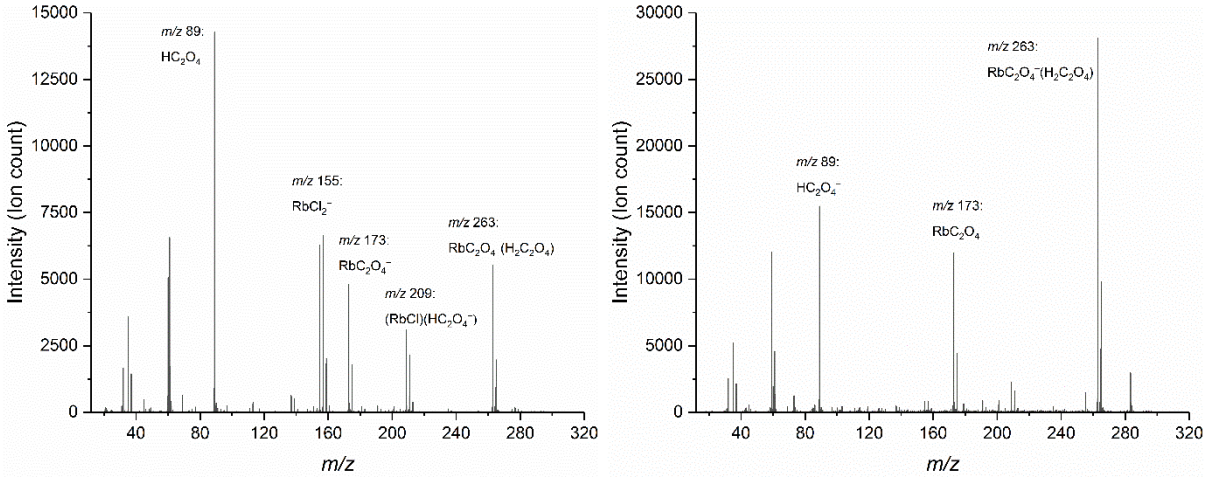

Figure S4. MS of 3.0 mM oxalic acid and 5.0 mM RbCl in 50/50 water/methanol (*left*), and of 3.0 mM oxalic acid and 5.0 mM RbCl in 50/50 water/methanol with 10% TEA (*right*).

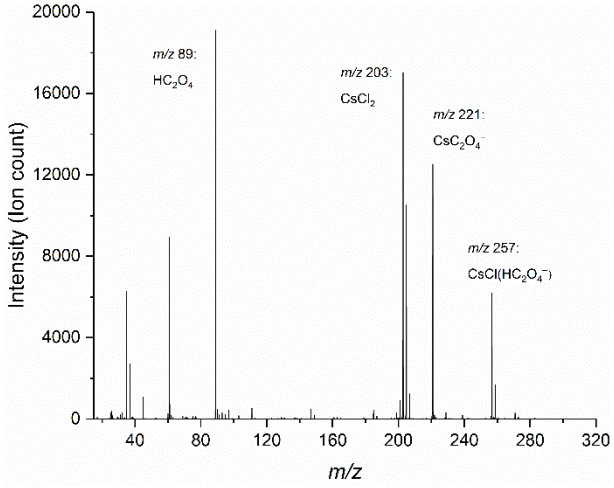

Figure S5. MS of 3.0 mM oxalic acid and 5.0 mM CsCl in 50/50 water/methanol.

SI-B. Validation of estimated threshold energies by known reaction energies

i. Dissociation of protonated ethanol, $C_2H_5OH_2^+$

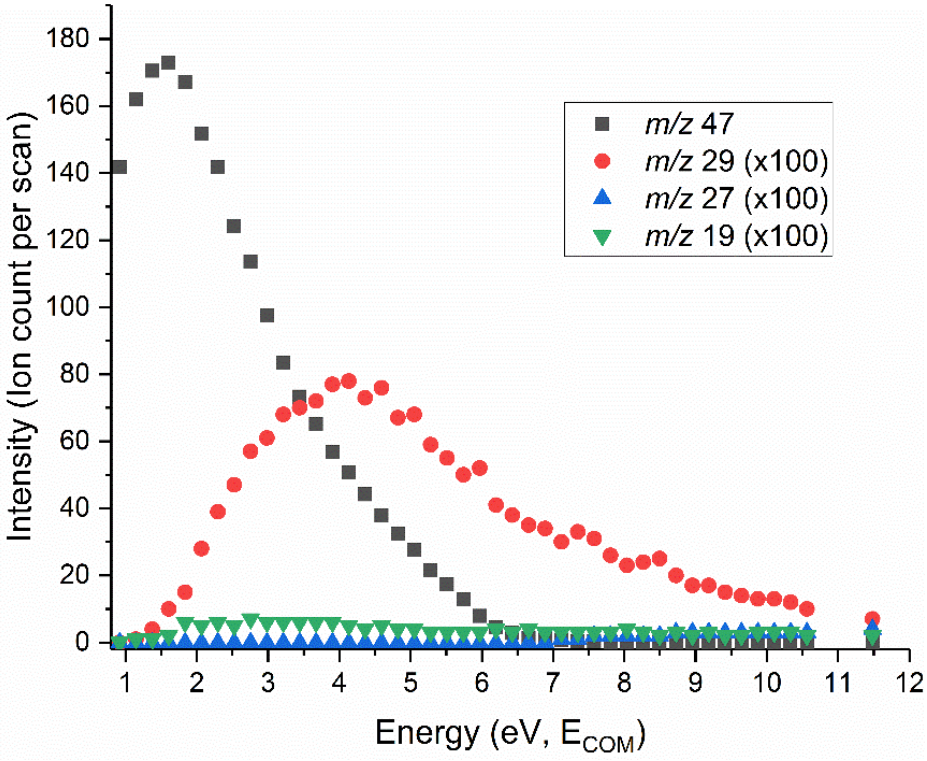

Figure S6. Breakdown curve of protonated ethanol, $C_2H_5OH_2^+$, *m/z* 47, recorded over a collision energy range from 0.9 to 11.5 eV (E_{COM}), 2.0 $\times 10^{-4}$ mbar Ar. *m/z* 29 corresponds to $C_2H_5^+$, *m/z* 27 to $C_2H_3^+$ and *m/z* 19 to H_3O^+. The intensities of the two smallest ions, *m/z* 19 and 27 were too low to yield reliable threshold energy estimates.

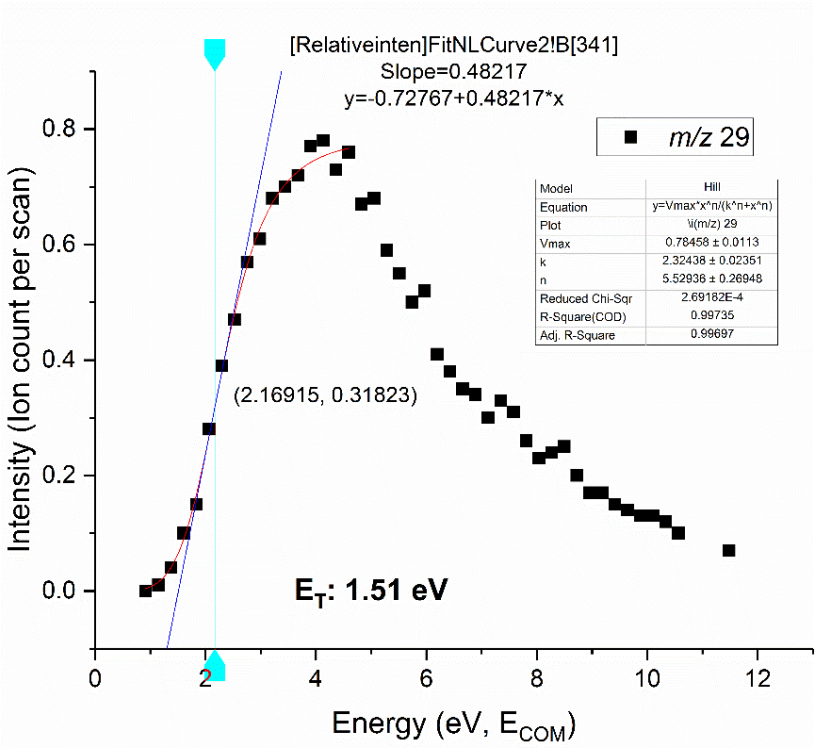

Figure S7. Appearance curve of ethyl cation, $C_2H_5^+$, *m/z* 29, recorded over a collision energy range from 0.9 to 11.5 eV (E_{COM}), $2.0 \cdot 10^{-4}$ mbar Ar. The curve has been fitted to a Hill function, and extrapolated to baseline in order to estimate the threshold energy (E_T) for its formation.

Table S1. Experimental and calculated reaction enthalpies ($\Delta_rH°$) and threshold energies (E_T) for $C_2H_5OH_2^+ \rightarrow C_2H_5^+ + H_2O$ in eV (kJ/mol in parentheses). Our estimate in **bold** (our calculations on the G4 level of theory, also in **bold**).

Exp		Calc	
$\Delta_rH°$	E_T	$\Delta_rH°$	E_T
	1.51 (146)		**1.45 (140)**
1.60 (154)[1]		1.48 (143)[1]	
	1.70 (164)[2]		1.76 (170)[3]

ii. Decarboxylation of benzoate, $C_6H_5CO_2^-$

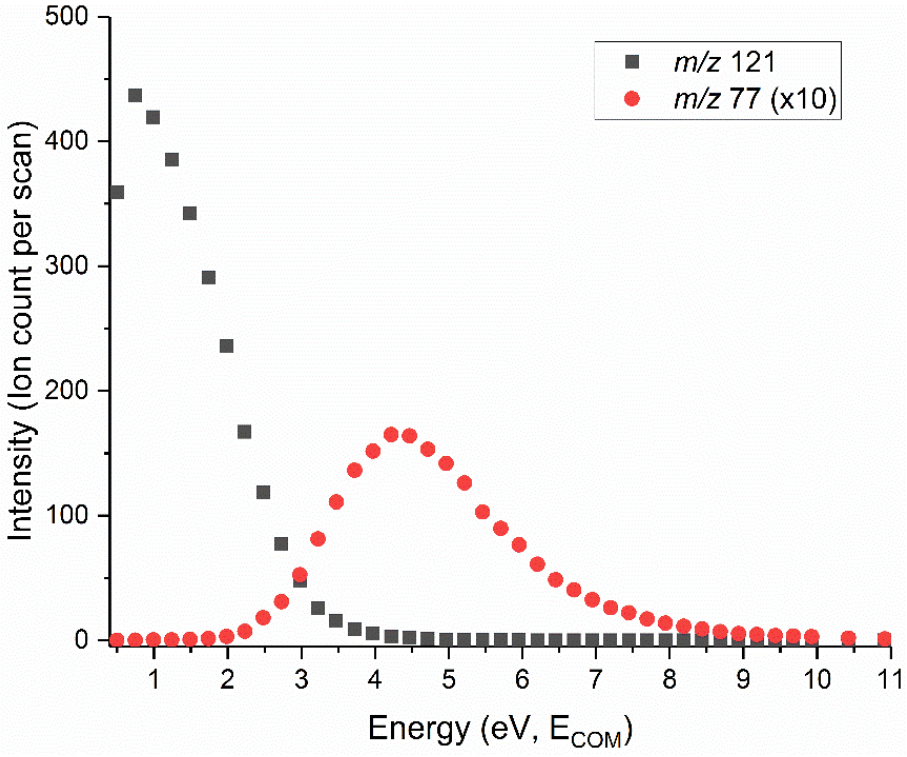

Figure S8. Breakdown curve of benzoate, $C_6H_5CO_2^-$, *m/z* 121, recorded over a collision energy range from 0.5 to 11.0 eV (E_{COM}), $2.0 \cdot 10^{-4}$ mbar Ar. *m/z* 77 corresponds to the product of decarboxylation, $C_6H_5^-$.

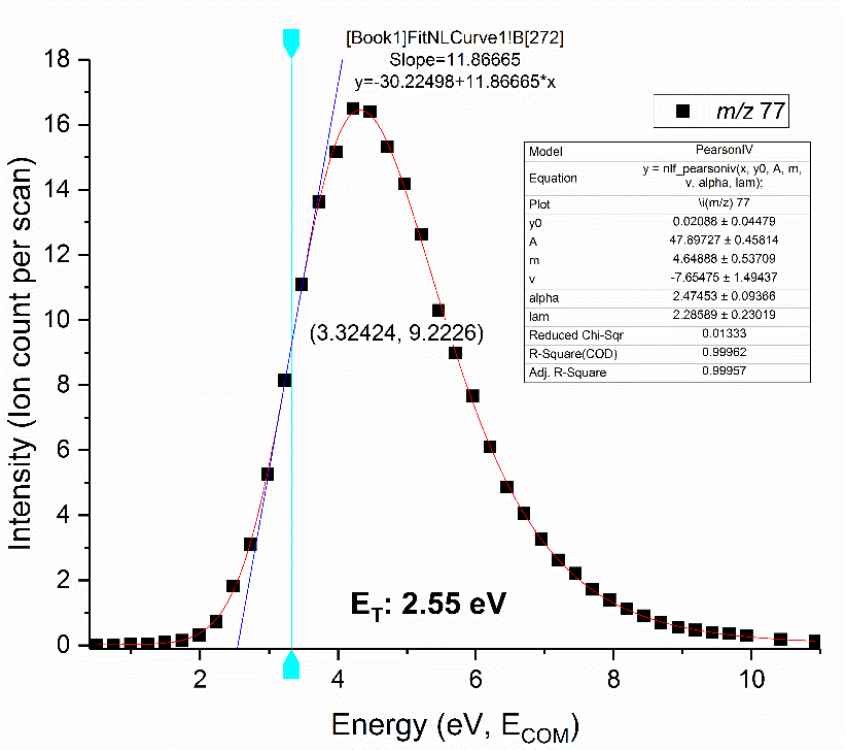

Figure S9. Appearance curve of the phenyl anion, $C_6H_5^-$, *m/z* 77, recorded over a collision energy range from 0.5 to 11.0 eV (E_{COM}), 2.0 · 10^{-4} mbar Ar. The curve has been fitted to a Pearson function, and extrapolated to baseline in order to estimate the threshold energy (E_T) for its formation.

Table S2. Experimental and calculated reaction enthalpies ($\Delta_rH°$) and threshold energies (E_T) for $C_6H_5CO_2^-$ → $C_6H_5^-$ + CO_2 in eV (kJ/mol in parentheses). Our estimate in **bold** (our calculations on the G4 level of theory, also in **bold**).

Exp		Calc	
$\Delta_rH°$	E_T	$\Delta_rH°$	E_T
	2.55 (246)		**2.43**
	2.63 ± 0.15 (254 ± 14)[4]		

SI-C. Molecular orbitals of the alkali metals and metal carbonites

The molecular orbital diagrams in this section were prepared using the Chemissian 4.52 software.[5]

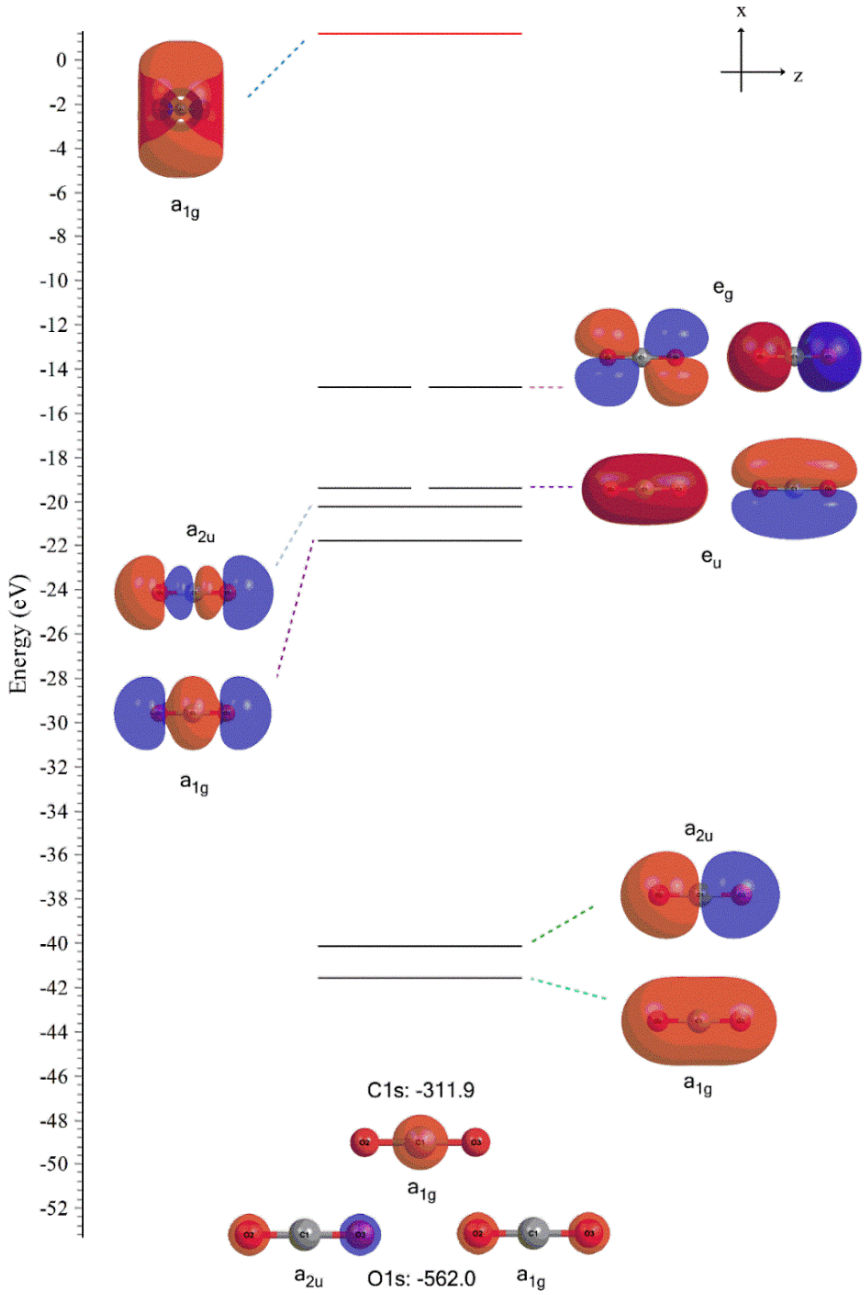

Figure S10. Molecular orbital diagram for CO_2 at the CCSD(T)/def2-TZVPPD optimized geometry (black lines = doubly occupied/red lines = virtual orbitals). The three lowest orbitals are frozen.

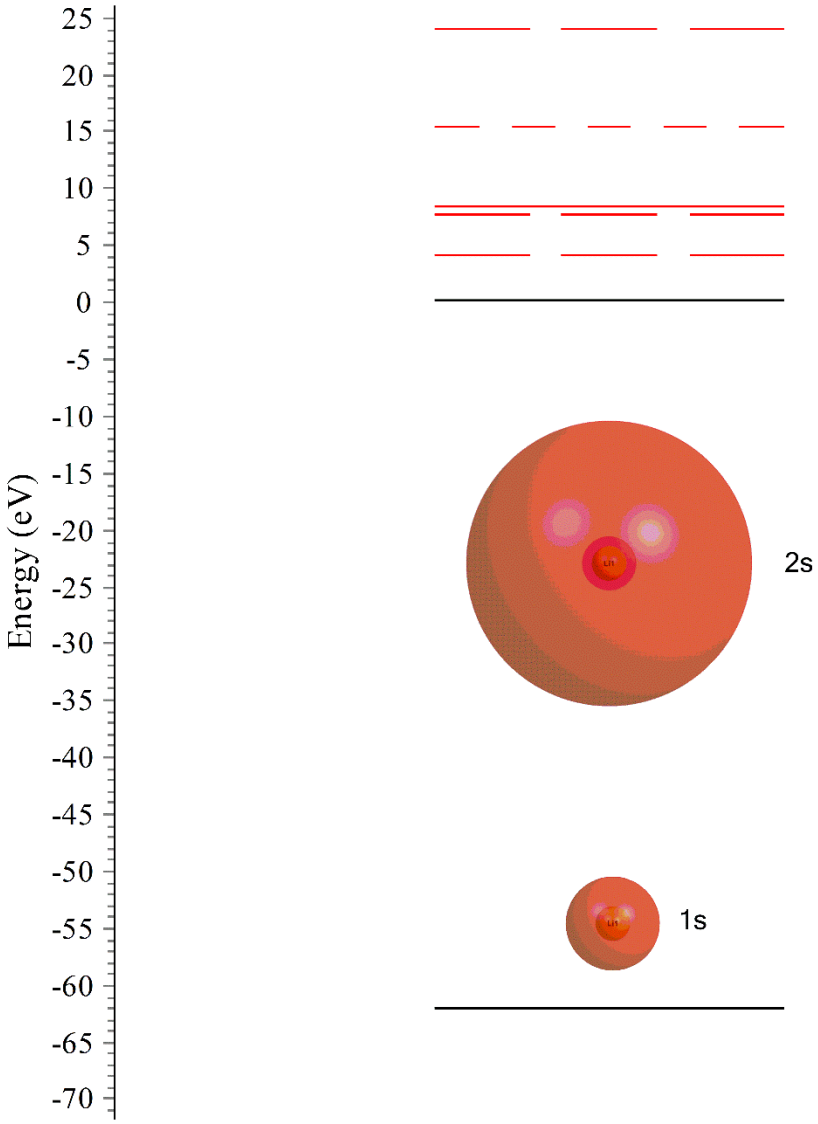

Figure S11. Atomic orbital diagram for Li^- computed at the CCSD(T)/def2-TZVPPD level of theory (black lines = doubly occupied/red lines = virtual orbitals). The 1s orbital is frozen in the frozen core approximation.

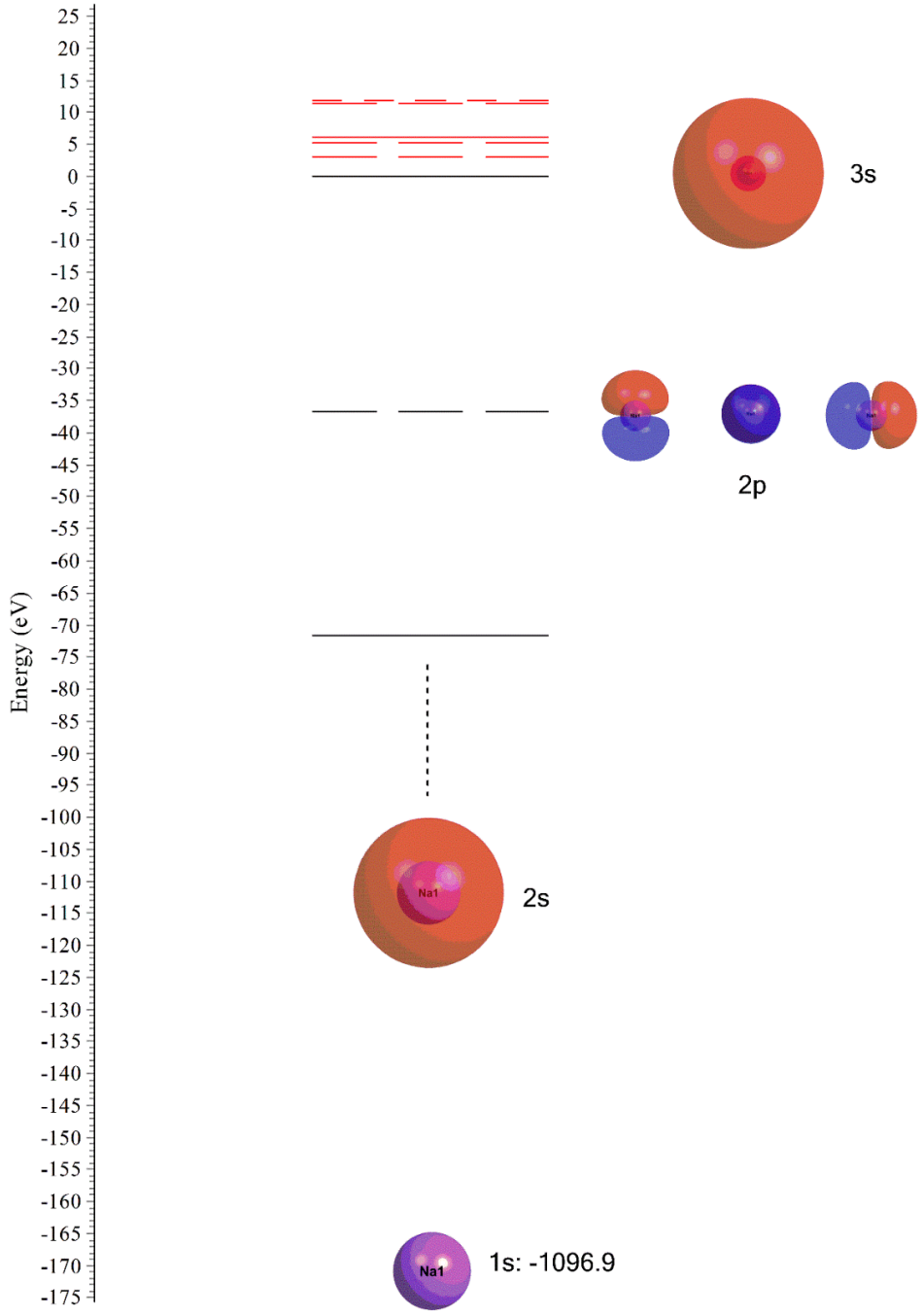

Figure S12. Atomic orbital diagram for Na^- computed at the CCSD(T)/def2-TZVPPD level of theory (black lines = doubly occupied/red lines = virtual orbitals). The five lowest orbitals are frozen in the frozen core approximation, while we have frozen the two lowest.

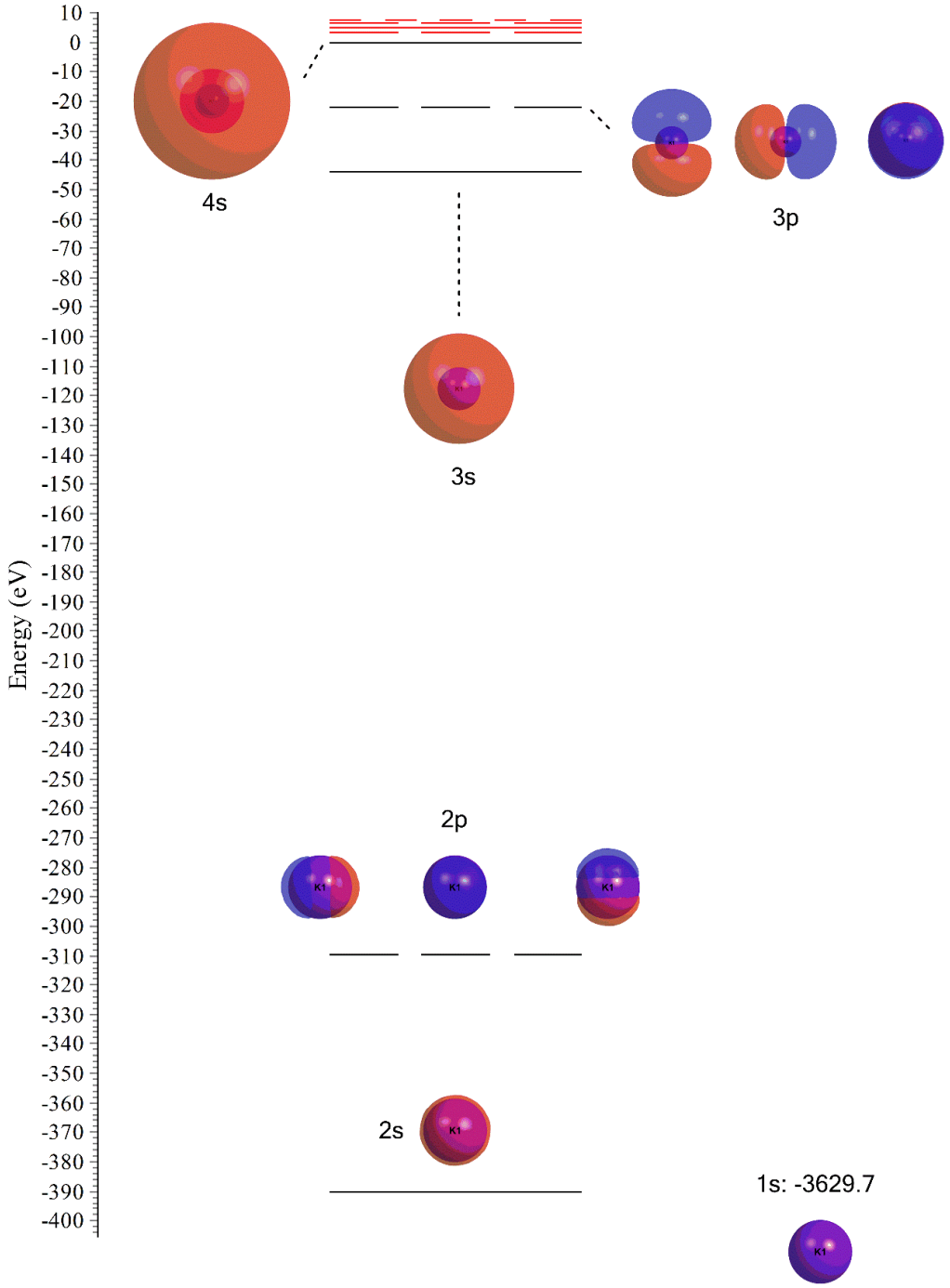

Figure S13. Atomic orbital diagram for K^- computed at the CCSD(T)/def2-TZVPPD level of theory (black lines = doubly occupied/red lines = virtual orbitals). The nine lowest orbitals are frozen in the frozen core approximation, while we have frozen the six lowest.

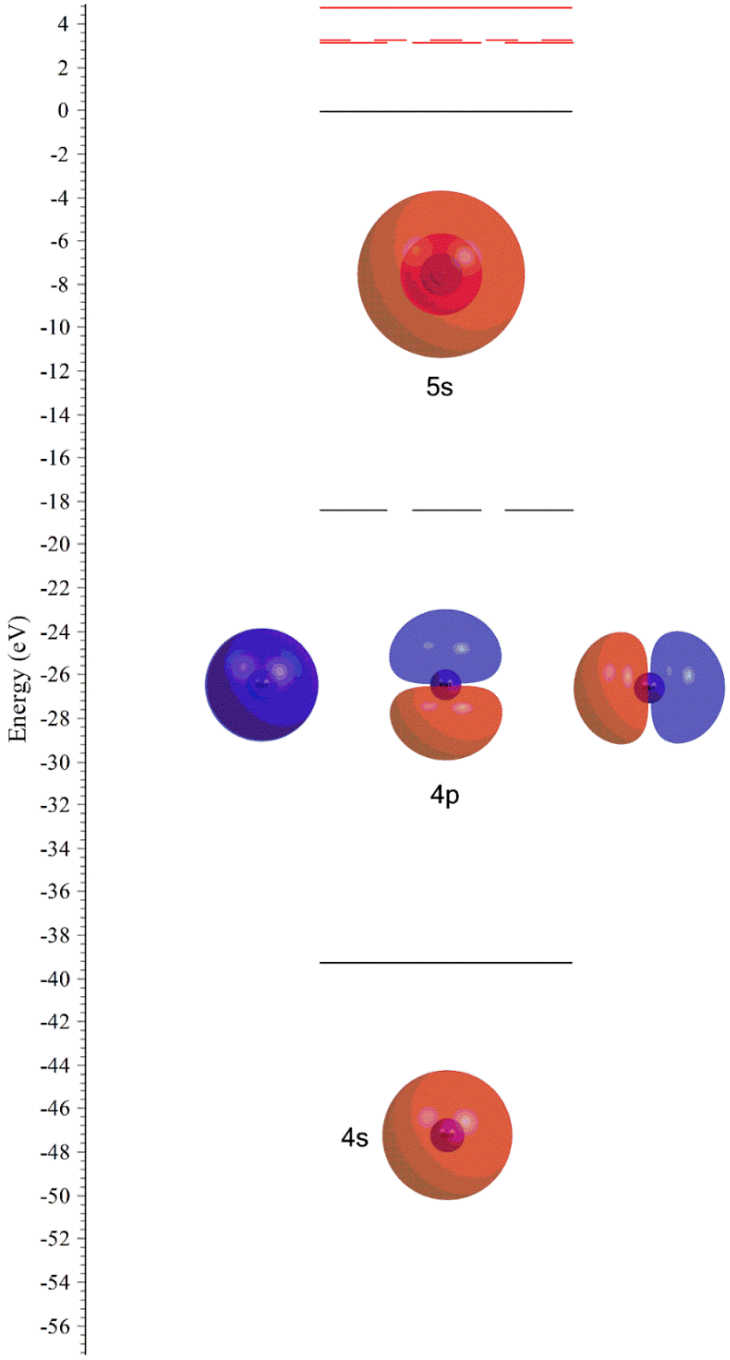

Figure S14. Atomic orbital diagram for Rb^- computed at the CCSD(T)/def2-TZVPPD level of theory (black lines = doubly occupied/red lines = virtual orbitals). The 28 inner electrons have been replaced by an ECP.

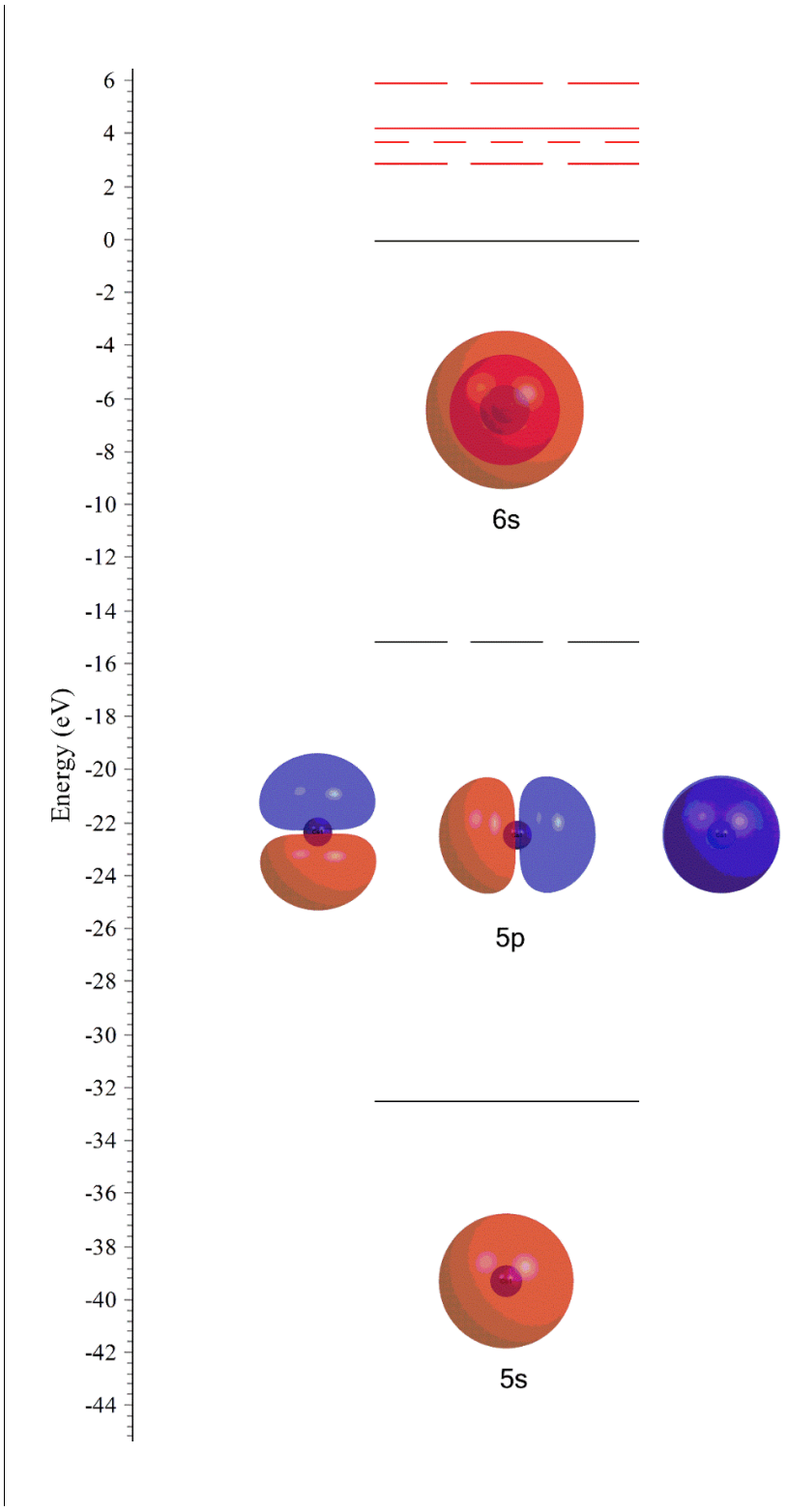

Figure S15. Atomic orbital diagram for Cs^- computed at the CCSD(T)/def2-TZVPPD level of theory (black lines = doubly occupied/red lines = virtual orbitals). The 46 inner electrons have been replaced by an ECP.

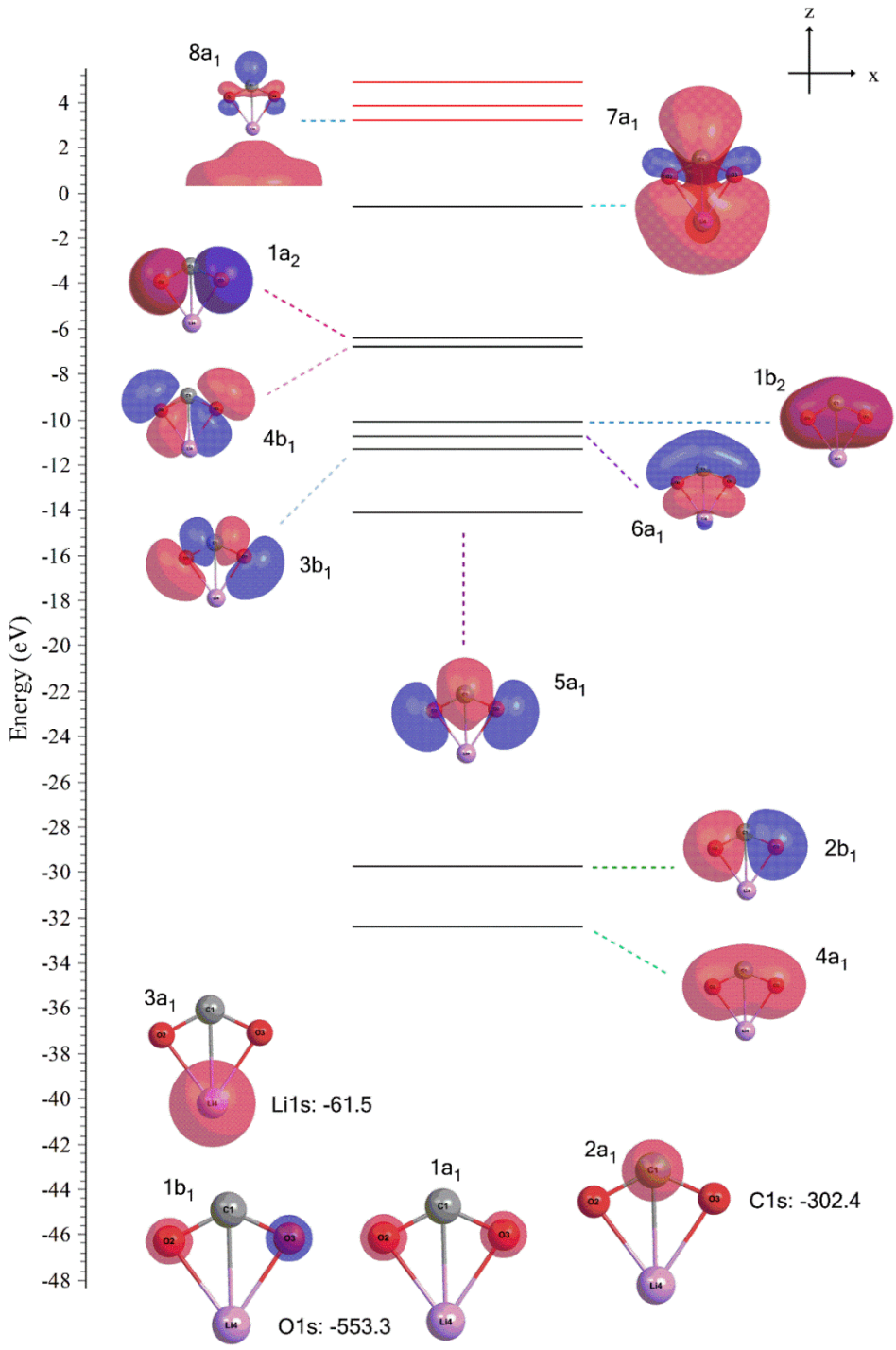

Figure S16. Molecular orbital diagram for Li(κ^2-O_2C)$^-$ (A isomer) at the CCSD(T)/def2-TZVPPD optimized geometry (black lines = doubly occupied/red lines = virtual orbitals). The four lowest orbitals are frozen.

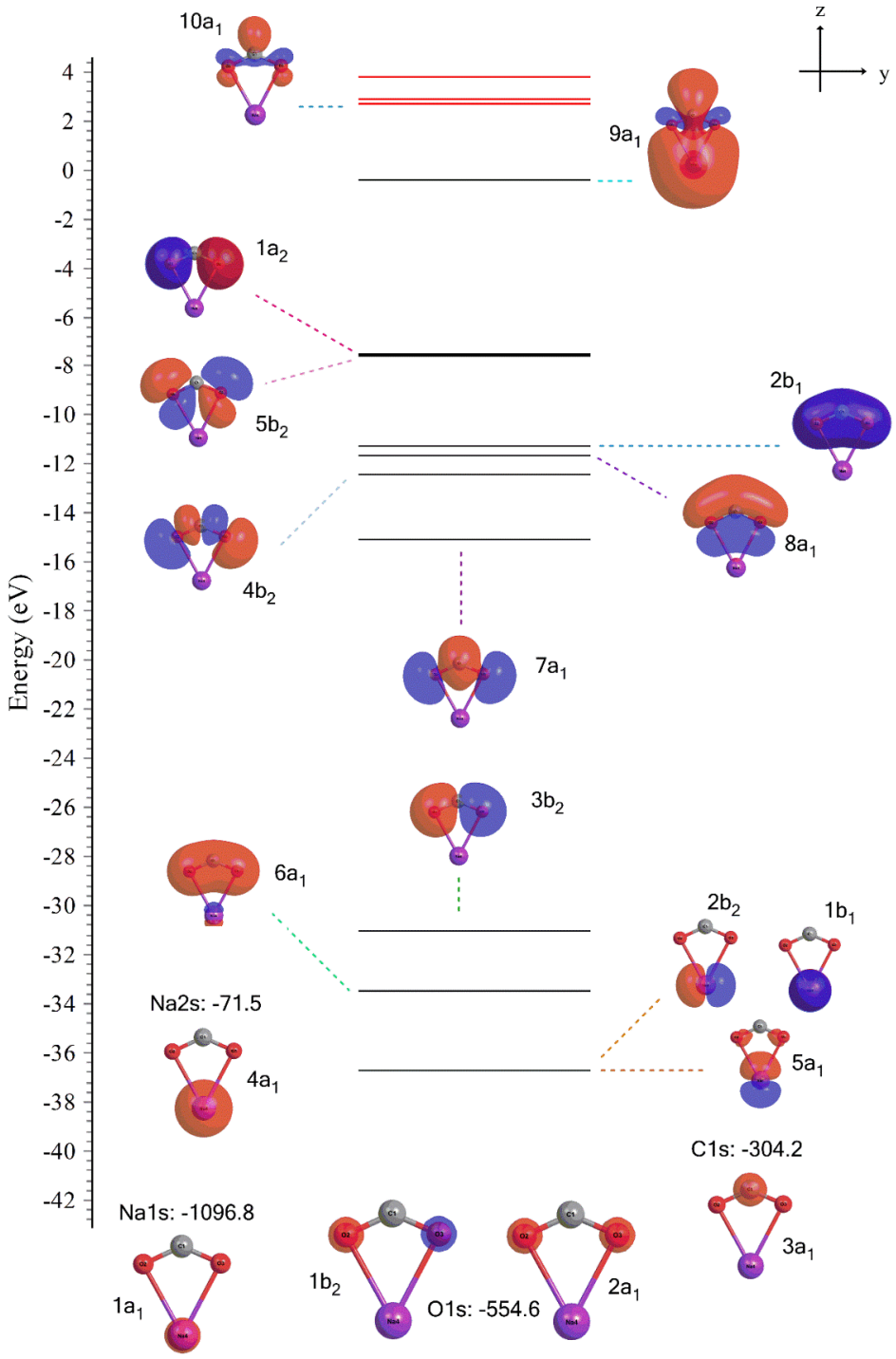

Figure S17. Molecular orbital diagram for $Na(\kappa^2\text{-}O_2C)^-$ (A isomer) at the CCSD(T)/def2-TZVPPD optimized geometry (black lines = doubly occupied/red lines = virtual orbitals). The eight lowest orbitals are frozen in the frozen core approximation, while we froze the five lowest orbitals.

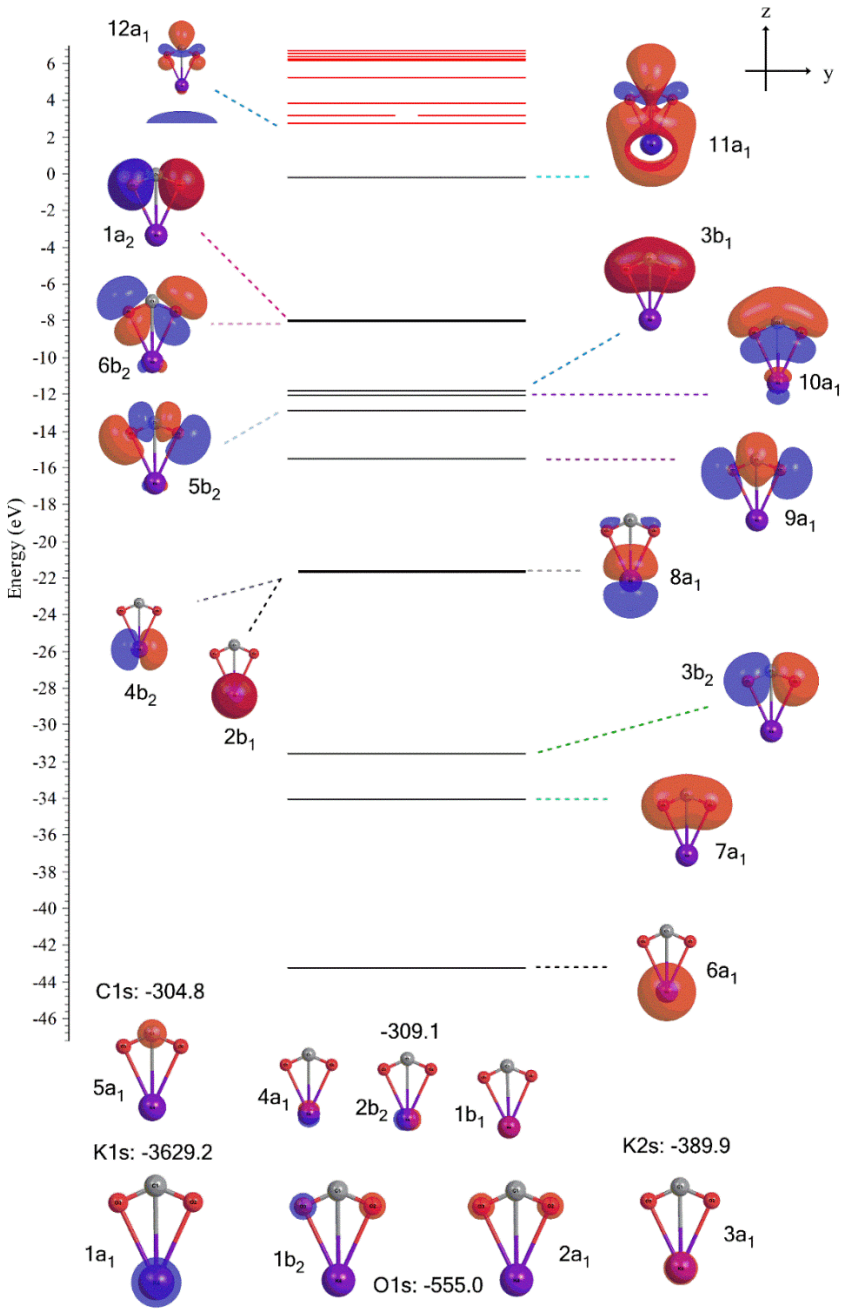

Figure S18. Molecular orbital diagram for $K(\kappa^2\text{-}O_2C)^-$ (A isomer) at the CCSD(T)/def2-TZVPPD optimized geometry (black lines = doubly occupied/red lines = virtual orbitals). The twelve lowest orbitals are frozen in the frozen core approximation, while we froze the nine lowest orbitals. Note how the carbon/oxygen 2s MOs ($7a_1$ and $3b_2$) are lower in energy than K 2p AOs ($2b_1$, $4b_2$ and $8a_1$).

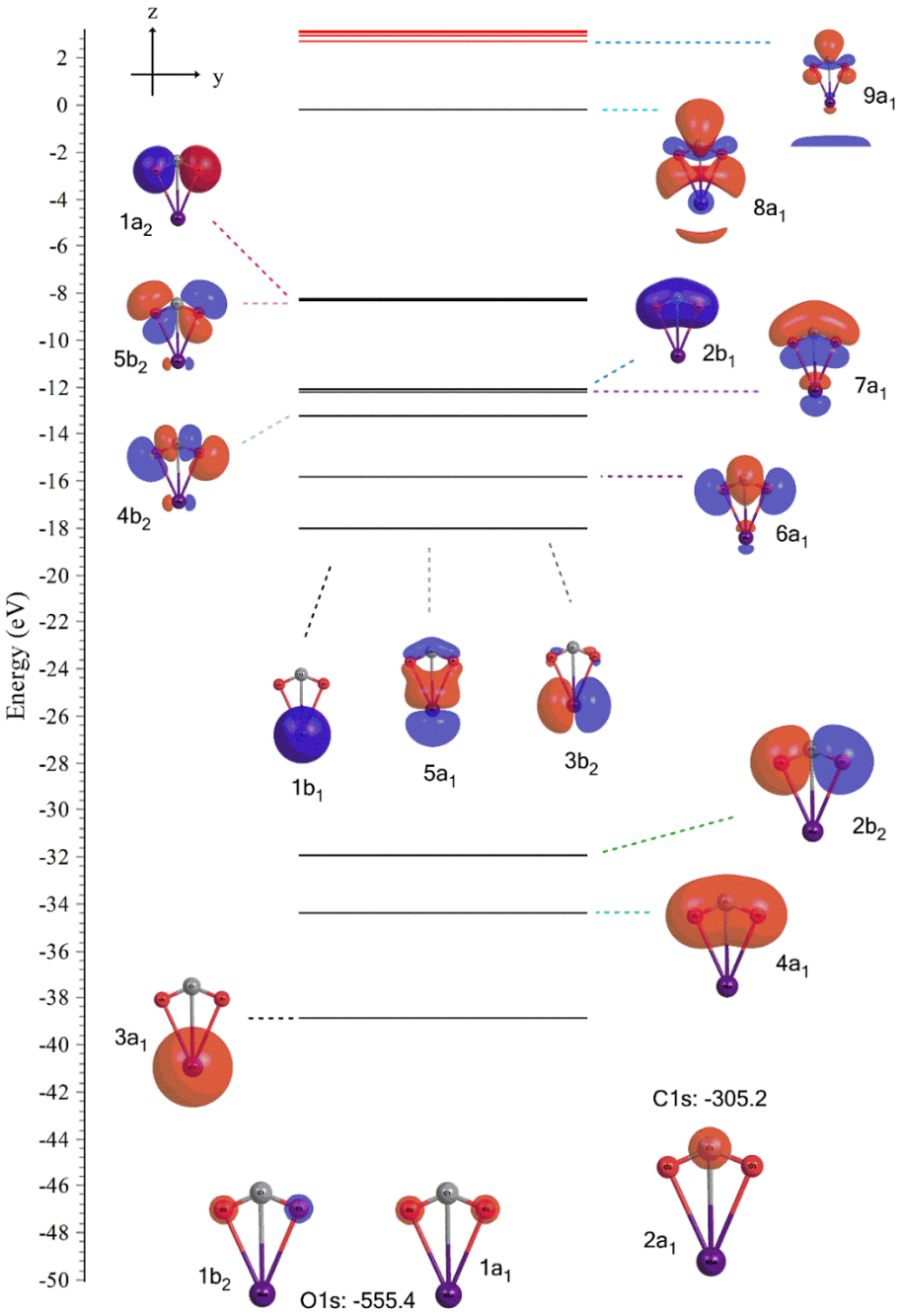

Figure S19. Molecular orbital diagram for $Rb(\kappa^2\text{-}O_2C)^-$ (A isomer) at the CCSD(T)/def2-TZVPPD optimized geometry (black lines = doubly occupied/red lines = virtual orbitals). The 28 inner electrons on Rb have been replaced by an ECP, and the three lowest orbitals are frozen in the complex.

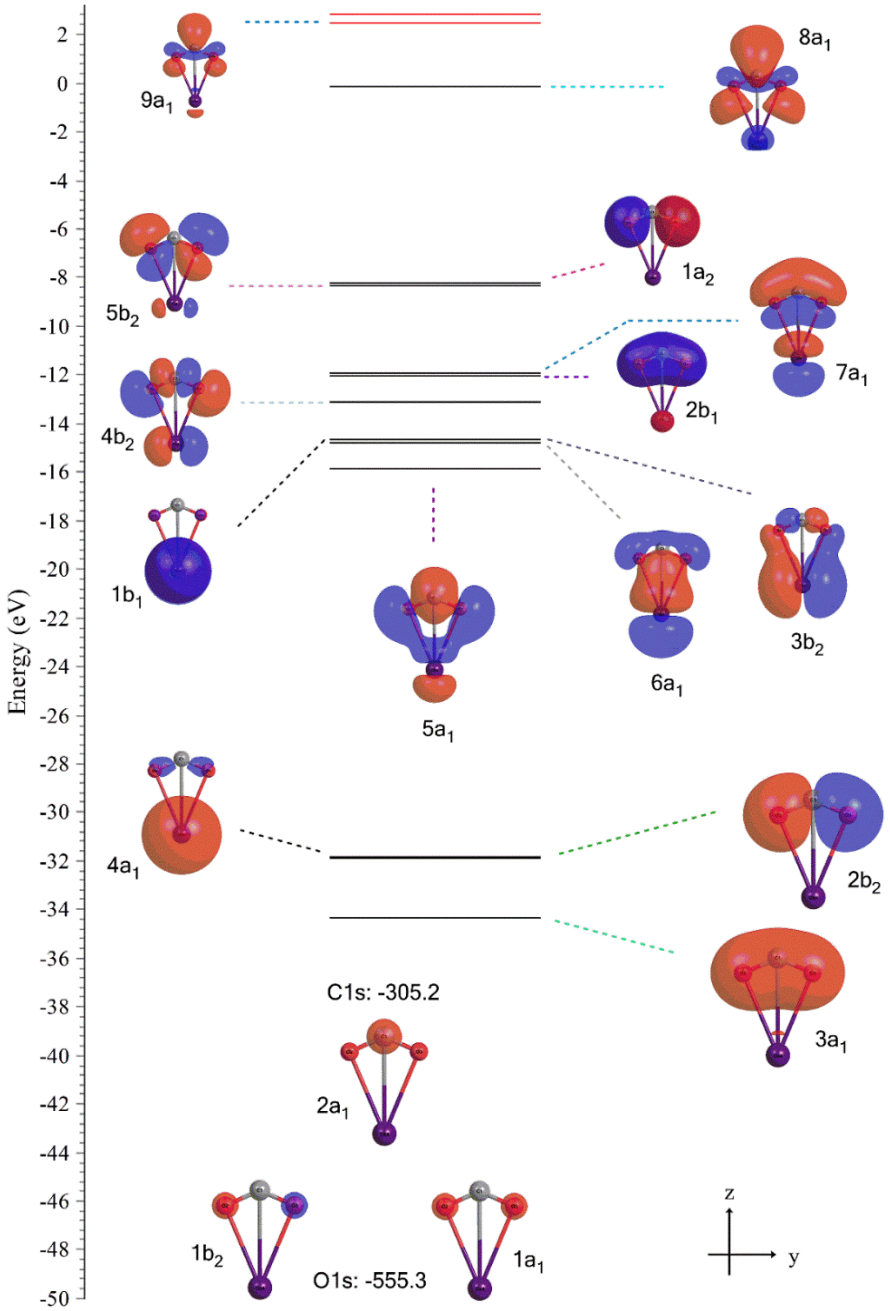

Figure S20. Molecular orbital diagram for $Cs(\kappa^2\text{-}O_2C)^-$ (A isomer) at the CCSD(T)/def2-TZVPPD optimized geometry (black lines = doubly occupied/red lines = virtual orbitals). The 46 inner electrons on Cs have been replaced by an ECP, and the three lowest orbitals are frozen in the complex,

SI-D. Calculation of the Basis Set Superposition Error (BSSE) correction

The uncorrected, ΔE, and BSSE-corrected, $\Delta E(BSSE)$, interaction energies are estimated using a procedure reported earlier[6] according to

$$\Delta E = E_{AB}^{\alpha\cup\beta}(AB) - E_A^{\alpha}(A) - E_B^{\beta}(B) \quad \text{(S1)}$$

$$\Delta E(BSSE) = \Delta E - \left\{E_{AB}^{\alpha\cup\beta}(A) - E_{AB}^{\alpha}(A)\right\} - \left\{E_{AB}^{\alpha\cup\beta}(B) - E_{AB}^{\beta}(B)\right\}, \quad \text{(S2)}$$

where $E_{AB}^{\alpha\cup\beta}(A)$ denotes the energy of fragment (*A*) in the dimer geometry *AB* using the combined basis sets of both the alkali metal (α) and the CO_2 fragment (β). The BSSE correction thus includes the deformation energy of the CO_2 fragment (*B*), which is substantial as the geometry of this fragment is bent in the dimer optimal geometry. Since fragment (*A*) is a monatomic cation, it is obvious that $E_{AB}^{\alpha}(A) = E_A^{\alpha}(A)$. i.e. its deformation energy is zero. The magnitudes of the various energy terms that are needed to estimate the uncorrected and BSSE-corrected interaction energies via equations (S1) and (S2) for isomers **A** and **B** for all alkali metal systems are listed in Tables S3 and S4.

Table S3. Energies (in a.u.) of the various terms of equations (S1) and (S2) needed to calculate the uncorrected and BSSE-corrected interaction energies of the **A isomer** of the alkali metal carbonites at the CCSD(T)/def2-TZVPPD level of theory. Here, the electronic energy of a molecule *M* at geometry *G* computed with basis set σ is defined as $E_G^{\sigma}(M)$. α is the basis set of the alkali metal, β is the basis set of CO_2 and $\alpha\cup\beta$ is the basis set of the dimer.

	$E_{MCO_2}^{\alpha\cup\beta}(MCO_2^-)$	$E_{CO_2}^{\beta}(CO_2)$	$E_M^{\alpha}(M^-)$	$E_{MCO_2}^{\alpha\cup\beta}(CO_2)$	$E_{MCO_2}^{\alpha\cup\beta}(M^-)$	$E_{MCO_2}^{\beta}(CO_2)$	ΔE	$\Delta E(BSSE)$
Li	−195.80034	−188.32603	−7.44970	−188.24346	−7.45194	−188.24294	−0.024615	−0.021861
Na	−350.33935	−188.32603	−162.00462	−188.25889	−162.00667	−188.25847	−0.008703	−0.006231

K	−787.64906	−188.32603	−599.31520	−188.26367	−599.31673	−188.26334	−0.007839	−0.005977
Rb	−212.26058	−188.32603	−23.92619	−188.26549	−23.93043	−188.26518	−0.008364	−0.003817
Cs	−208.36501	−188.32603	−20.02985	−188.26315	−20.03317	−188.2629	−0.009135	−0.005547

Table S4. Energies (in a.u.) of the various terms of equations (S1) and (S2) needed to calculate the uncorrected and BSSE-corrected interaction energies of the **B isomer** of the alkali metal carbonites at the CCSD(T)/def2-TZVPPD level of theory. Here, the electronic energy of a molecule *M* at geometry *G* computed with basis set σ is defined as $E_G^{\sigma}(M)$. α is the basis set of the alkali metal, β is the basis set of CO_2 and $\alpha \cup \beta$ is the basis set of the dimer.

	$E_{MCO_2}^{\alpha\cup\beta}(MCO_2^-)$	$E_{CO_2}^{\beta}(CO_2)$	$E_M^{\alpha}(M^-)$	$E_{MCO_2}^{\alpha\cup\beta}(CO_2)$	$E_{MCO_2}^{\alpha\cup\beta}(M^-)$	$E_{MCO_2}^{\beta}(CO_2)$	ΔE	$\Delta E(BSSE)$
Li	−195.79613	−188.32603	−7.44970	−188.26631	−7.45179	−188.26583	−0.020404	−0.017833
Na	−350.33193	−188.32603	−162.00462	−188.28015	−162.00647	−188.27978	−0.001286	0.000933
K	−787.64231	−188.32603	−599.31520	−188.28129	−599.3165	−188.28101	−0.001091	0.000508
Rb	−212.25331	−188.32603	−23.92619	−188.28245	−23.92974	−188.28219	−0.001097	0.002713
Cs	−208.35816	−188.32603	−20.02985	−188.28062	−20.03268	−188.28039	−0.002282	0.000781

Table S5. Uncorrected [ΔE] and BSSE-Corrected [$\Delta E(BSSE)$**]** (in parentheses) interaction energies (kJ/mol) for both **A** and **B** alkali metal carbonite isomers at the CCSD(T)/def2-TZVPPD level of theory.

	A	**B**
Li	−64.6 (−57.4)	−53.6 (−46.8)
Na	−22.9 (−16.4)	−3.4 (2.4)
K	−20.6 (−15.7)	−2.9 (1.3)
Rb	−22.0 (−10.0)	−2.9 (7.1)
Cs	−24.0 (−14.6)	−6.0 (2.1)

SI-E. Computational modeling of the unimolecular MOx^- dissociation

A detailed computational survey was conducted to aid the understanding of the elementary reaction steps constituting the full dissociation of metal oxalates into metal anions and carbon dioxide, the results of which were used to construct the potential energy diagrams in this section.

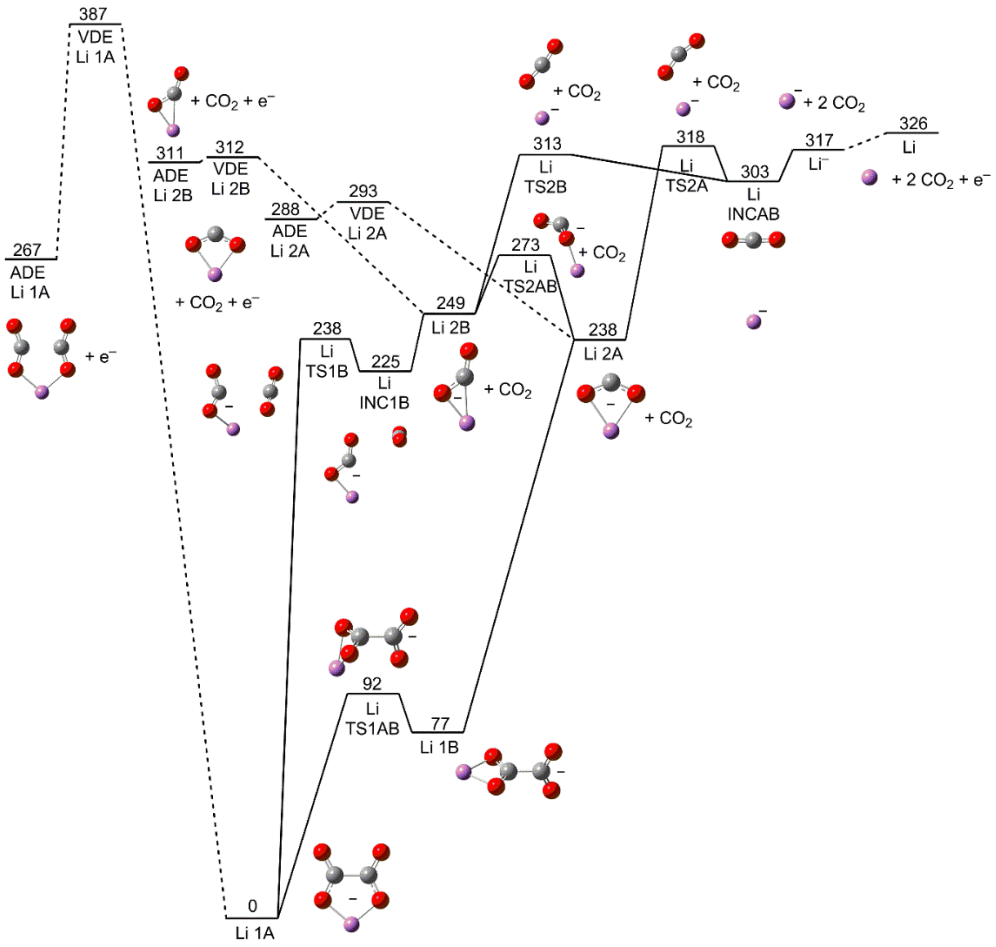

Figure S21. MP2/Def2-TZVPPD potential energy diagram for the dissociation of $LiC_2O_4^-$. The numbers are zero-point corrected electronic energies. Electron detachment of the MCO_2^- species is indicated by dashed (---) lines, while chemical transformations are drawn with full lines (—).

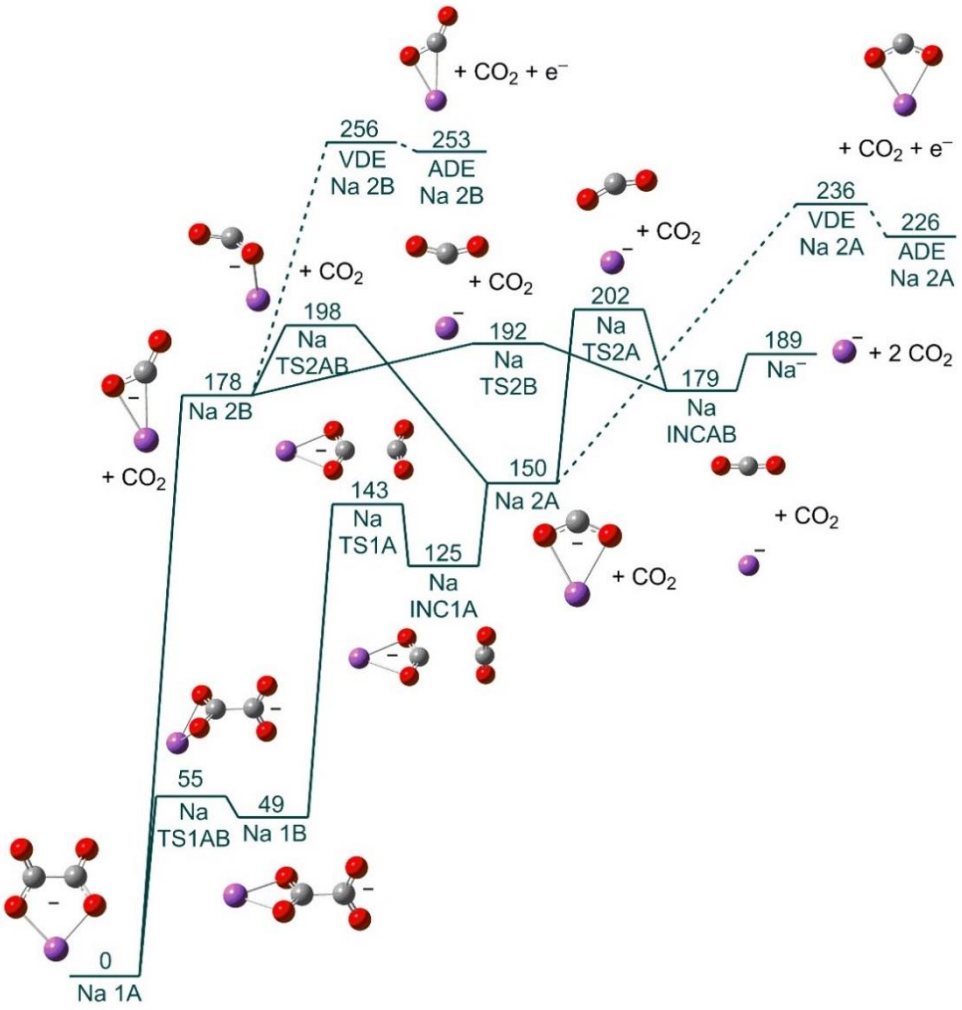

Figure S22. MP2/Def2-TZVPPD potential energy diagram for the dissociation of $NaC_2O_4^-$. The numbers are zero-point corrected electronic energies. Electron detachment of the MCO_2^- species is indicated by dashed (---) lines, while chemical transformations are drawn with full lines (—).

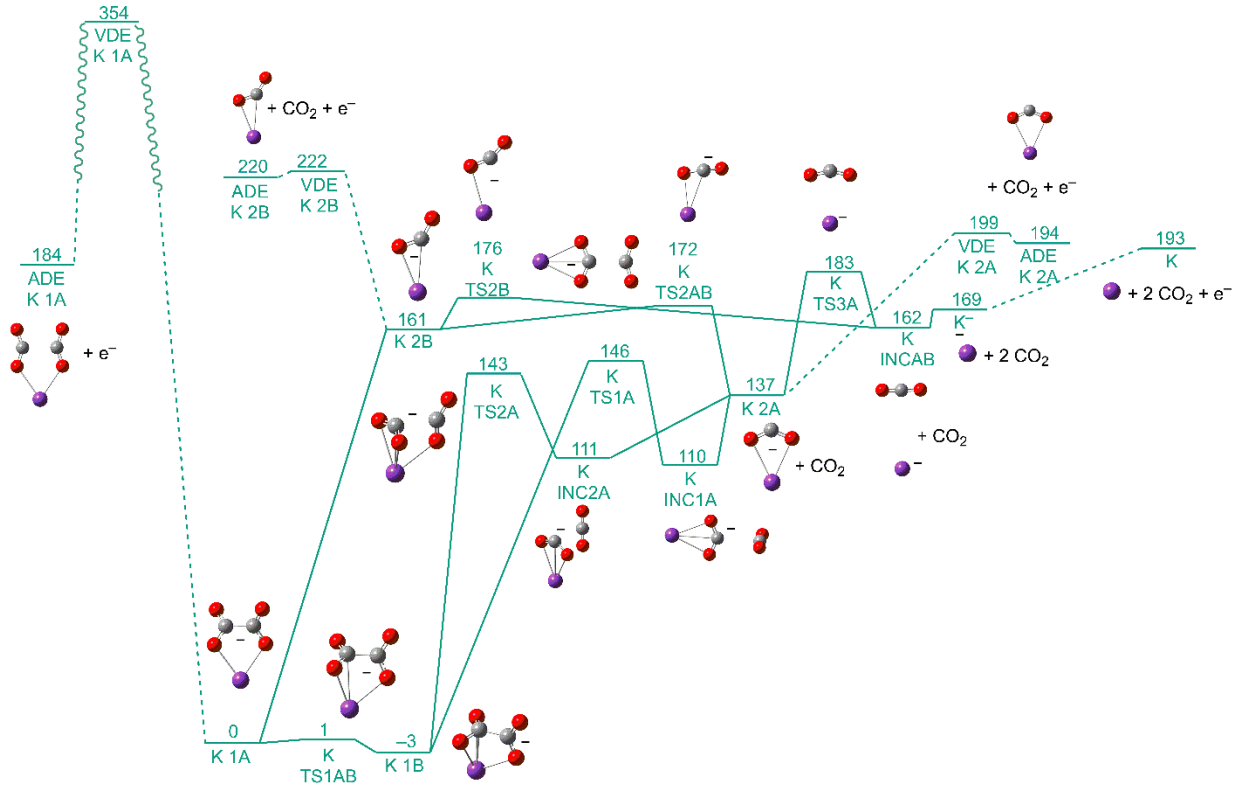

Figure S23. MP2/Def2-TZVPPD potential energy diagram for the dissociation of $KC_2O_4^-$. The numbers are zero-point corrected electronic energies. Electron detachment of the MCO_2^- species is indicated by dashed (---) lines, while chemical transformations are drawn with full lines (—).

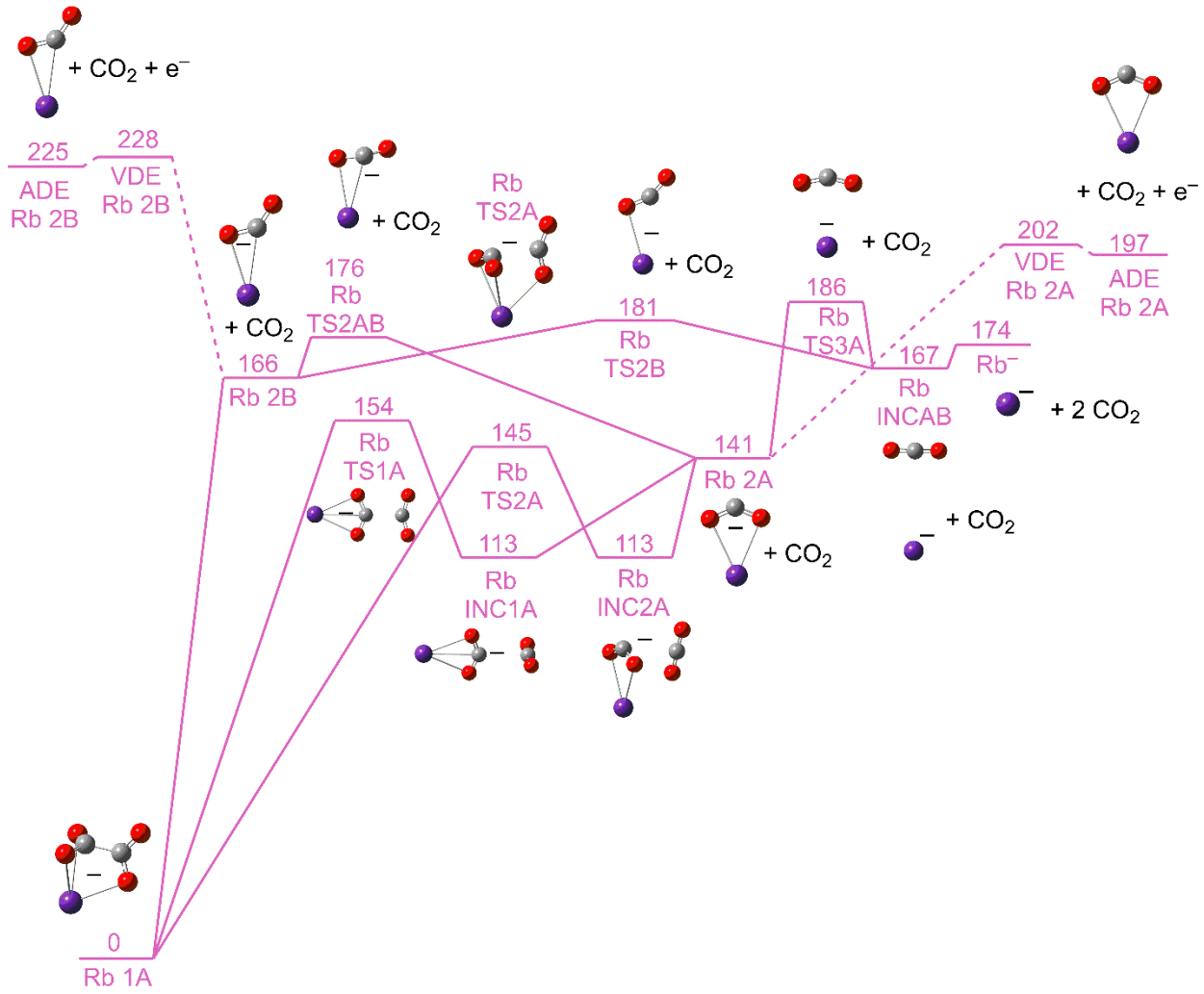

Figure S24. MP2/Def2-TZVPPD potential energy diagram for the dissociation of $RbC_2O_4^-$. The numbers are zero-point corrected electronic energies. Electron detachment of the MCO_2^- species is indicated by dashed (---) lines, while chemical transformations are drawn with full lines (—).

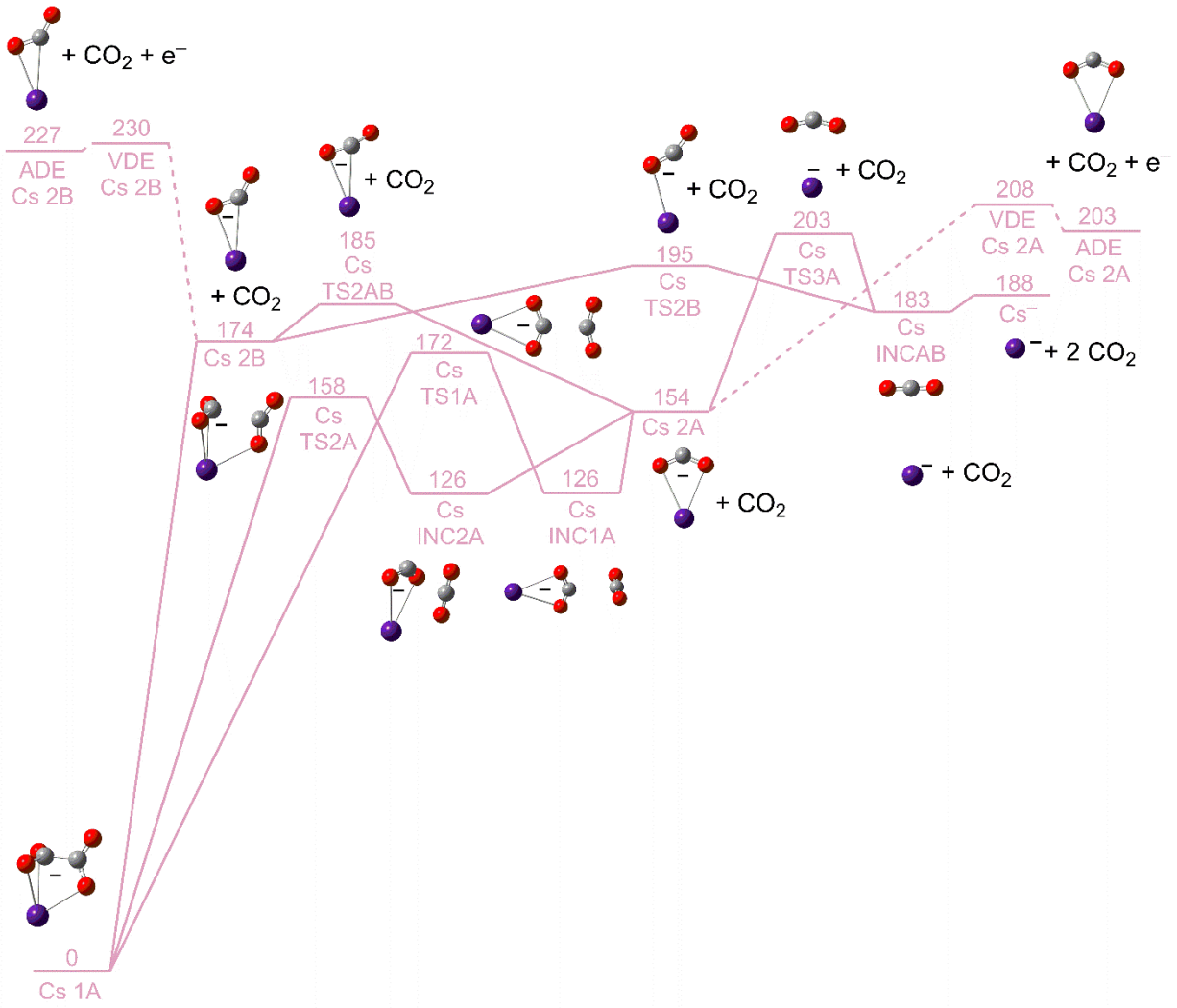

Figure S25. MP2/Def2-TZVPPD potential energy diagram for the dissociation of $CsC_2O_4^-$. The numbers are zero-point corrected electronic energies. Electron detachment of the MCO_2^- species is indicated by dashed (---) lines, while chemical transformations are drawn with full lines (—).

SI-F. Relative stabilities of the oxalate dianion conformers in different solvents

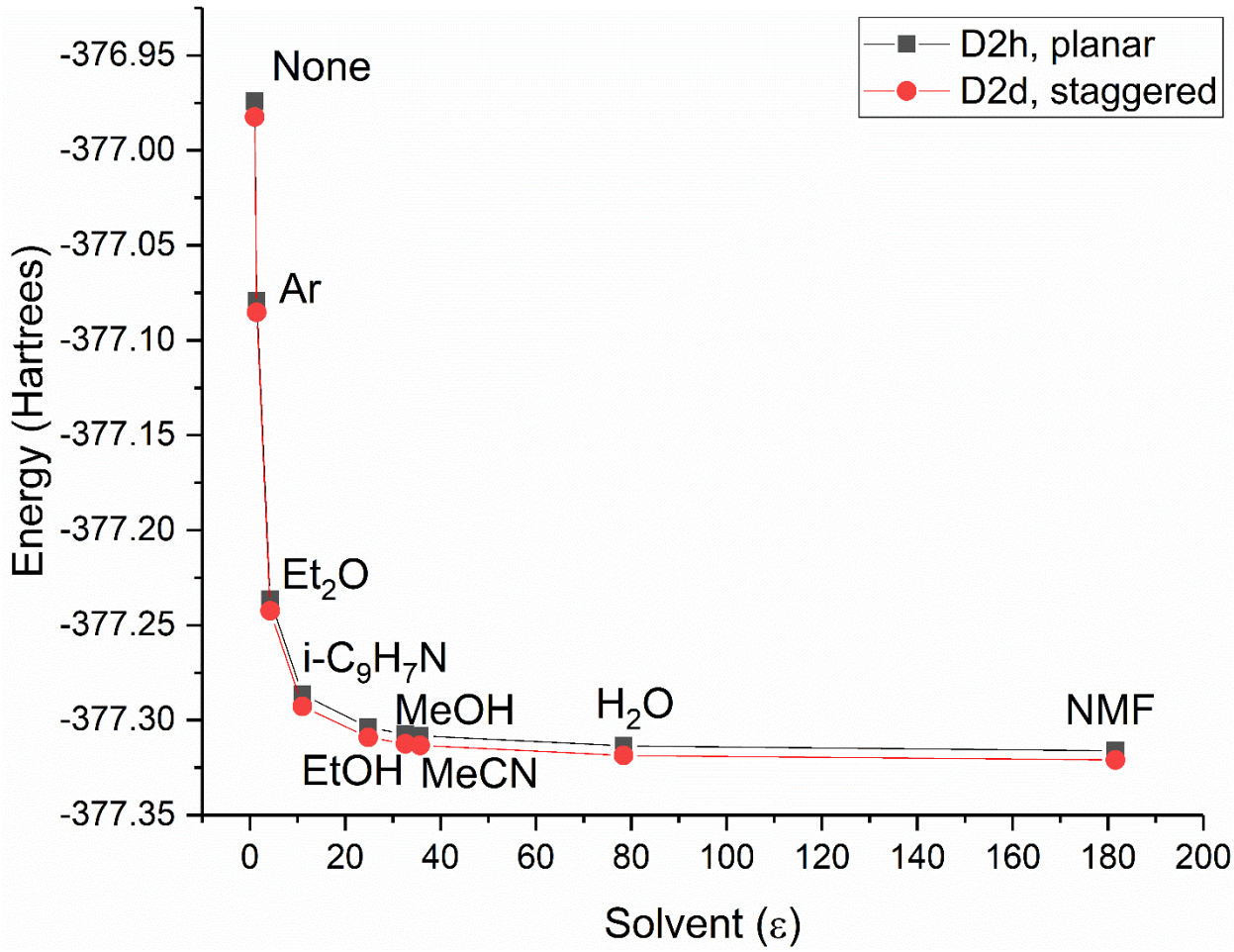

Figure S26. Stabilities of the staggered and planar Ox^{2-} by solvent on the MP2/def2-TZVPPD level of theory.

SI-G. Alkali metal carbonite (MCO_2^-) C(1s) energies and carboxylation barriers

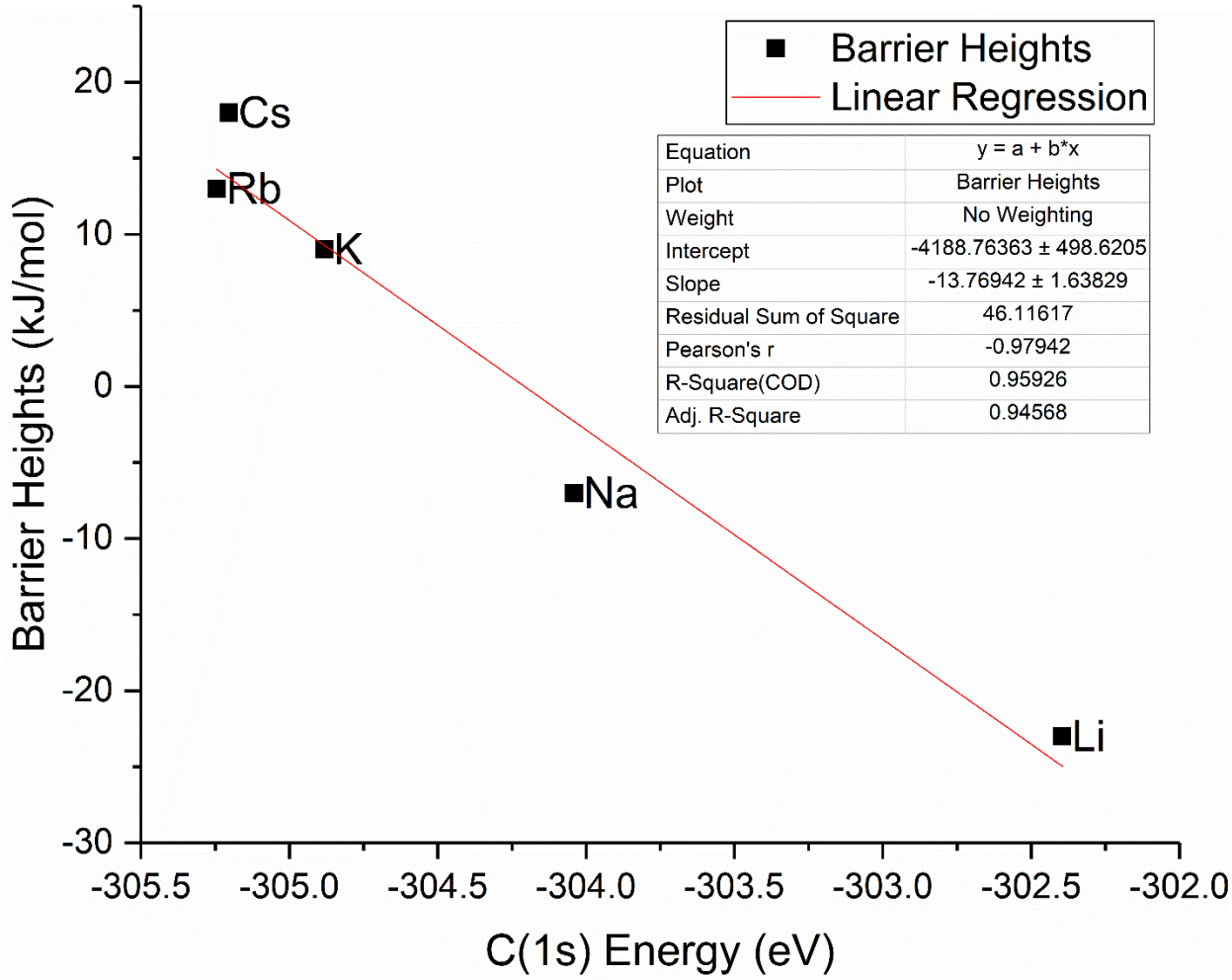

Figure S27. Correlation between the alkali metal carbonite (MCO_2^-) C(1s) energy and the barrier heights for CO_2 addition.

SI-H. Alkali metal oxalate crystal structures

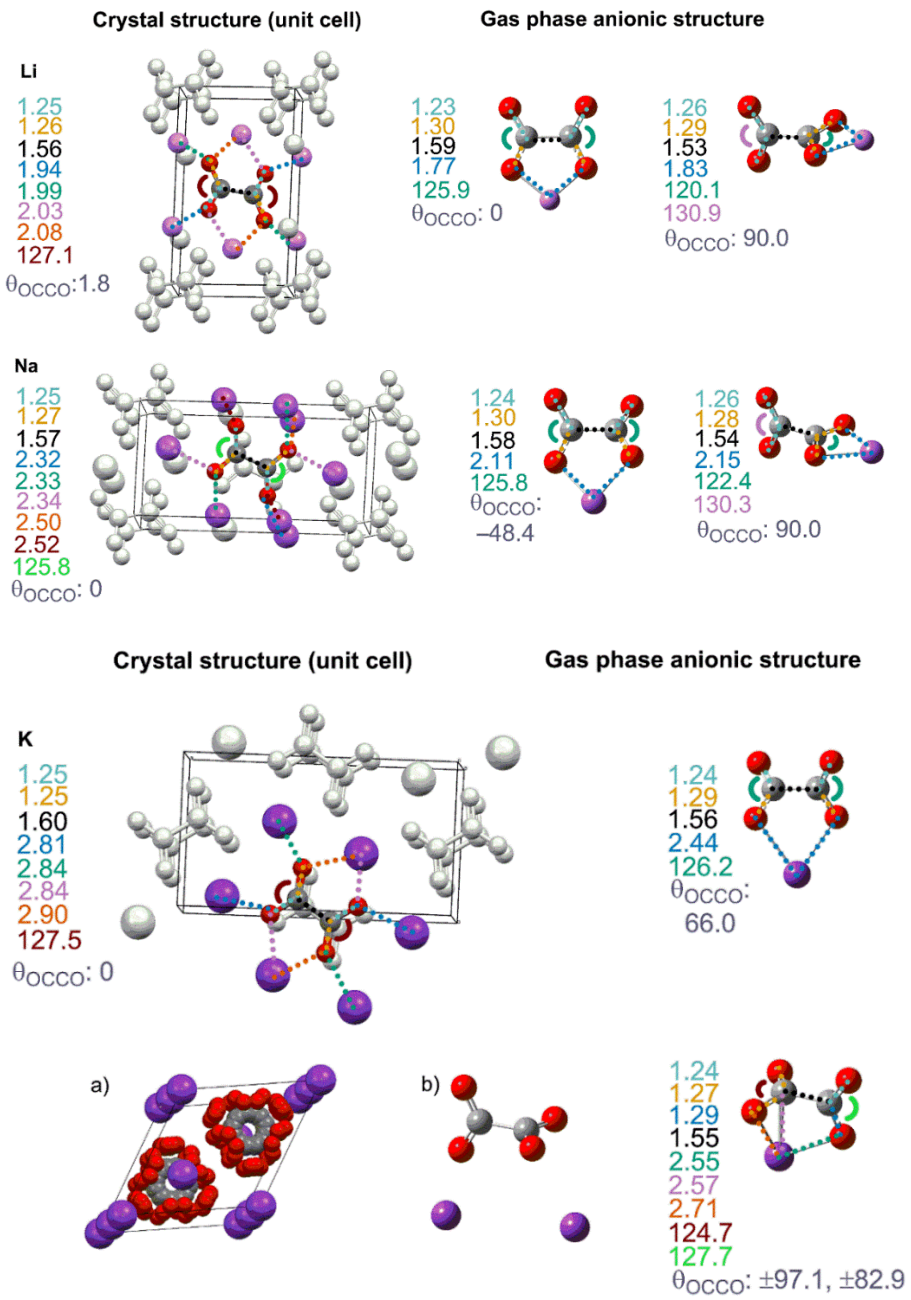

Figure S28. Reported crystal structures and computed MP2/def2-TZVPPD gas-phase ion structures for the alkali metal oxalates (Li – K).

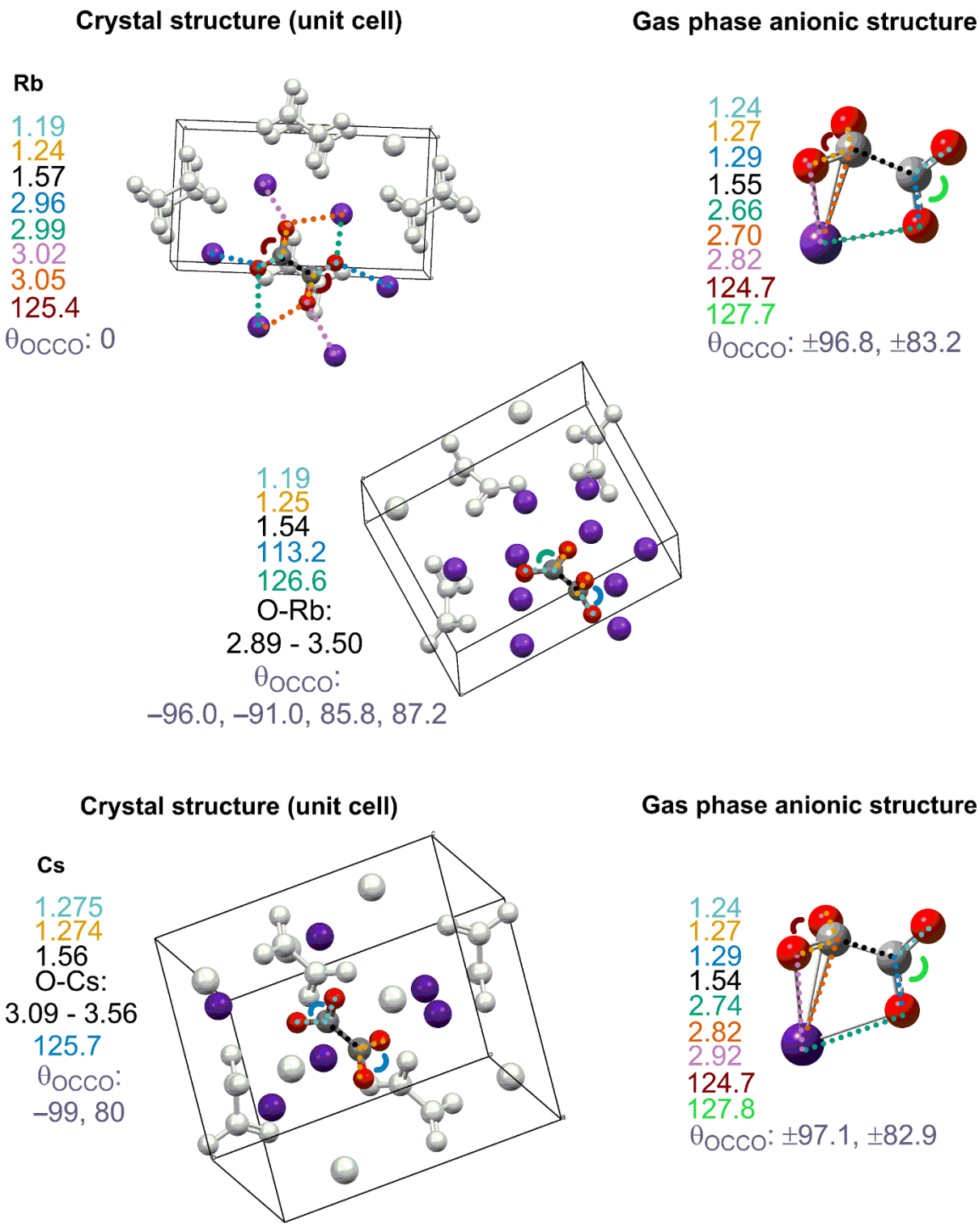

Figure S29. Reported crystal structures and computed MP2/def2-TZVPPD gas-phase ion structures for the alkali metal oxalates (Rb – Cs).

SI-I. Calculated [MP2/def2-TZVPPD] and observed IR spectra for $MC_2O_4^-$

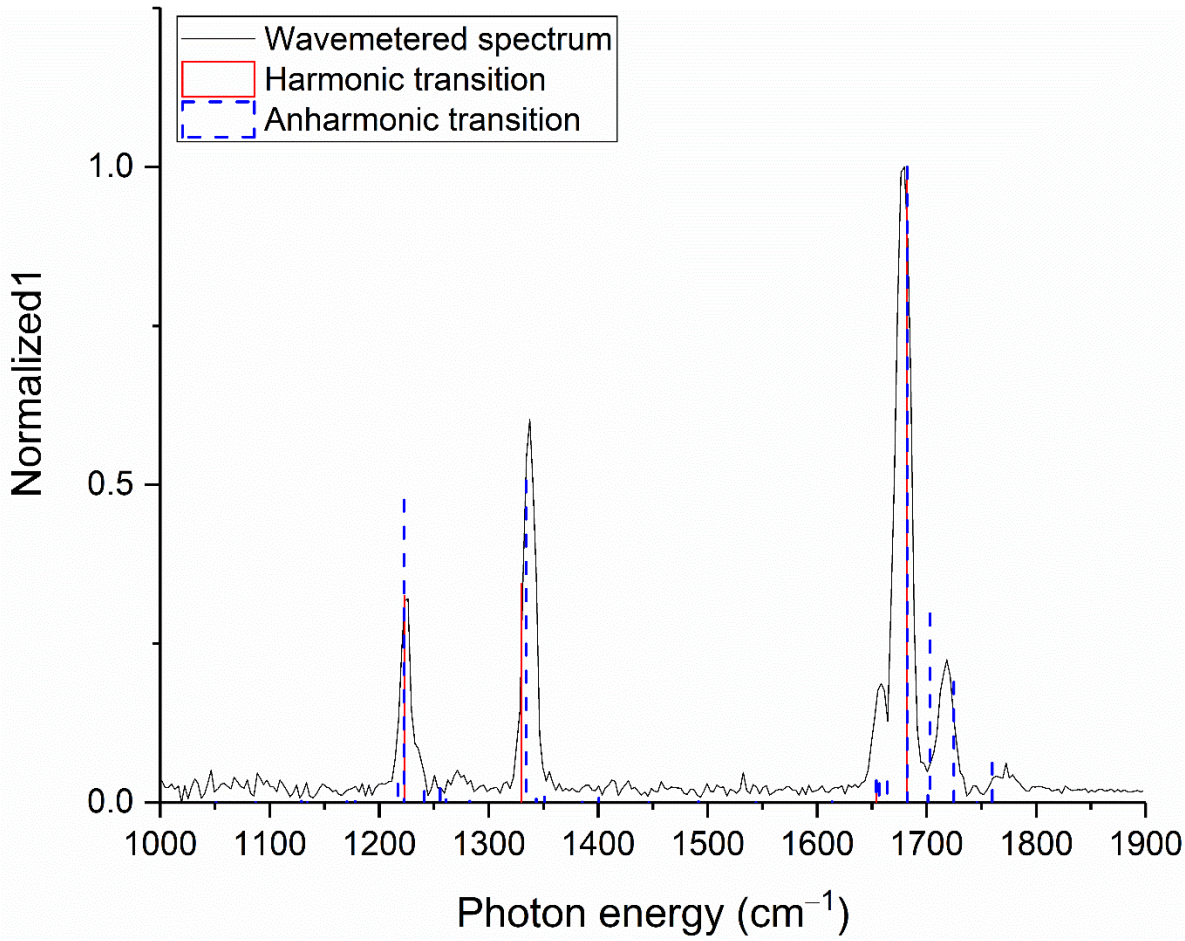

Figure S30. Calculated [MP2/def2-TZVPPD] vs. observed IR-spectra for $LiOx^-$.

Table S6. Calculated [MP2/def2-TZVPPD] and observed transitions for $LiOx^-$.

Description	Normal mode	Calculated transition (cm^{-1})	Scaled (×0.99) transition (cm^{-1})	Observed transition (cm^{-1})
Out-of-phase bound C=O stretch	ν_{12}	1235.36	1223.01	1219.96
In-phase bound C=O stretch	ν_{13}	1343.36	1329.93	1334.68
Out-of-phase unbound C=O stretch	ν_{14}	1670.67	1653.97	1661.11
In-phase unbound C=O stretch	ν_{15}	1698.96	1681.97	1682.86

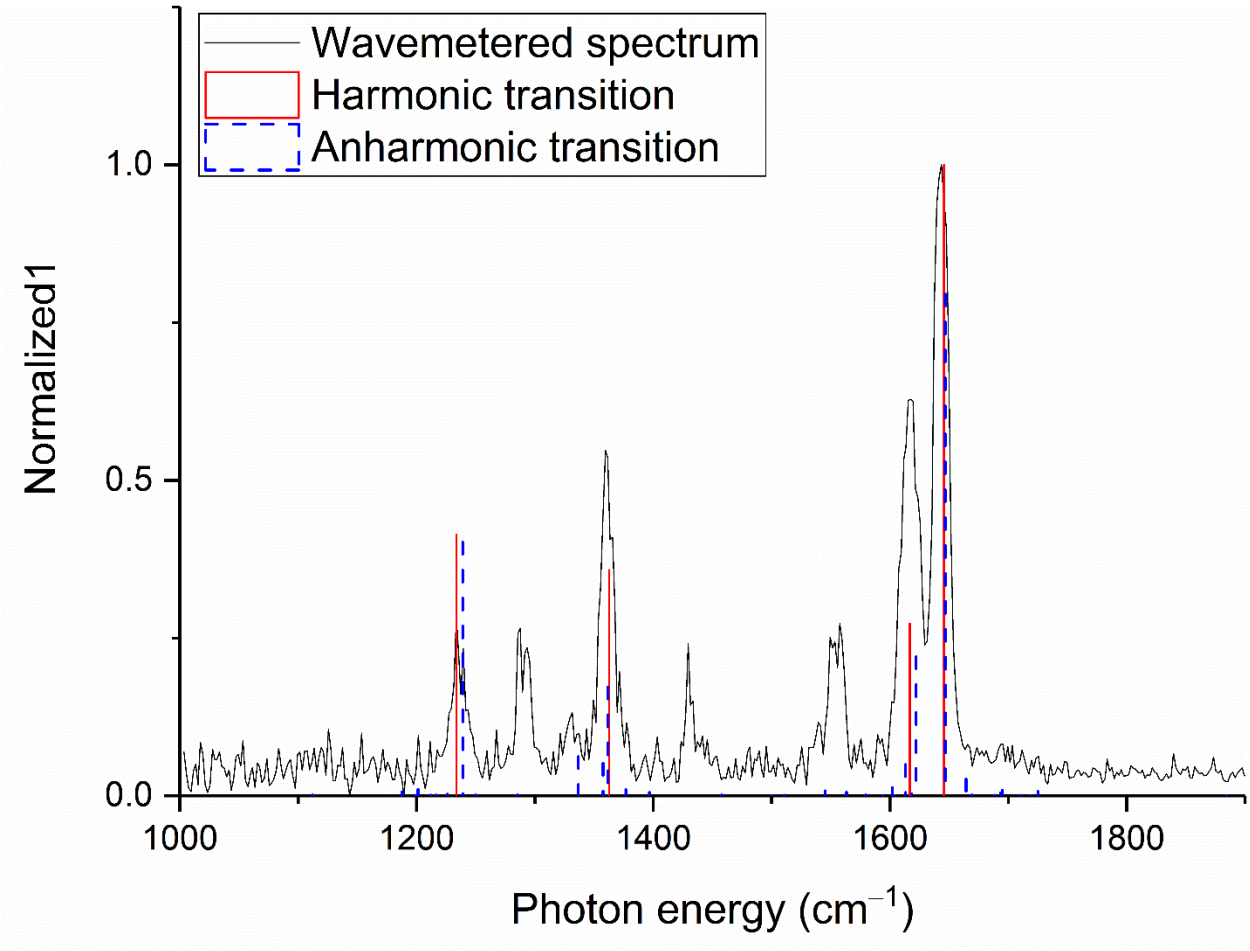

Figure S31. Calculated [MP2/def2-TZVPPD] vs. observed IR-spectra for $NaOx^-$.

Table S7. Calculated [MP2/def2-TZVPPD] and observed transitions for $NaOx^-$.

Description	Normal mode	Calculated transition (cm^{-1})	Scaled (×0.99) transition (cm^{-1})	Observed transition (cm^{-1})
Out-of-phase bound C=O stretch	ν_{12}	1246.27	1233.81	1232.46
In-phase bound C=O stretch	ν_{13}	1376.49	1362.72	1358.13
Out-of-phase unbound C=O stretch	ν_{14}	1633.11	1616.78	1624.62
In-phase unbound C=O stretch	ν_{15}	1662.17	1645.54	1651.57

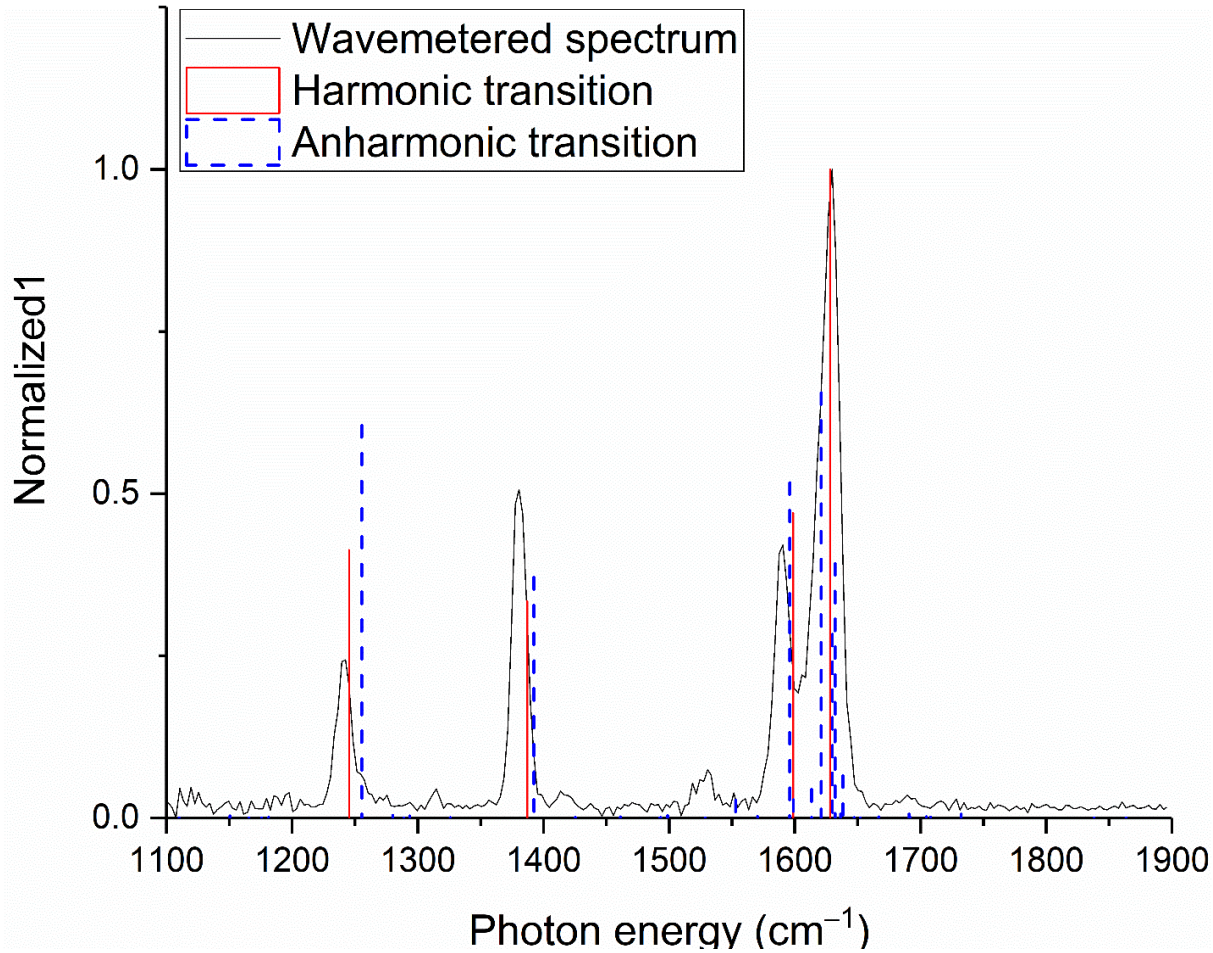

Figure S32. Calculated [MP2/def2-TZVPPD] vs. observed IR-spectra for KOx^-.

Table S8. Calculated [MP2/def2-TZVPPD] and observed transitions for KOx^-.

Description	Normal mode	Calculated transition (cm^{-1})	Scaled (×0.99) transition (cm^{-1})	Observed transition (cm^{-1})
Out-of-phase bound C=O stretch	ν_{12}	1257.86	1245.29	1238.45
In-phase bound C=O stretch	ν_{13}	1401.10	1387.09	1380.96
Out-of-phase unbound C=O stretch	ν_{14}	1614.80	1598.65	1591.95
In-phase unbound C=O stretch	ν_{15}	1644.55	1628.11	1634.49

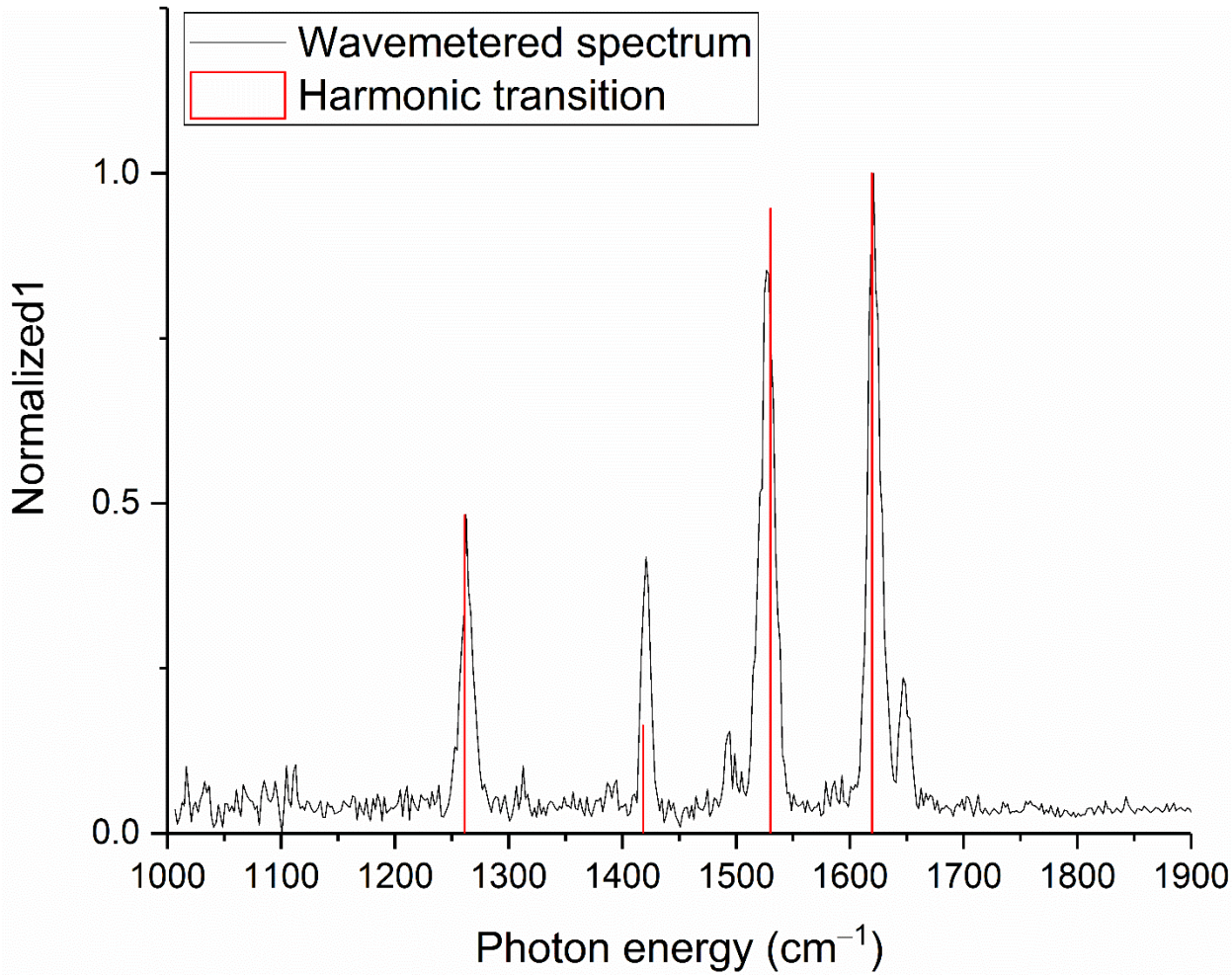

Figure S33. Calculated [MP2/def2-TZVPPD] vs. observed IR-spectra for $RbOx^-$.

Table S9. Calculated [MP2/def2-TZVPPD] and observed transitions for $RbOx^-$.

Description	Normal mode	Calculated transition (cm^{-1})	Scaled (×0.985) transition (cm^{-1})	Observed transition (cm^{-1})
Out-of-phase bound C=O and symmetric CO_2 stretch	ν_{12}	1280.41	1261.20	1250.65
In-phase bound C=O and symmetric CO_2 stretch	ν_{13}	1439.79	1418.20	1424.82
Antisymmetric CO_2 stretch	ν_{14}	1553.61	1530.30	1528.18
Unbound C=O stretch	ν_{15}	1644.12	1619.46	1622.89

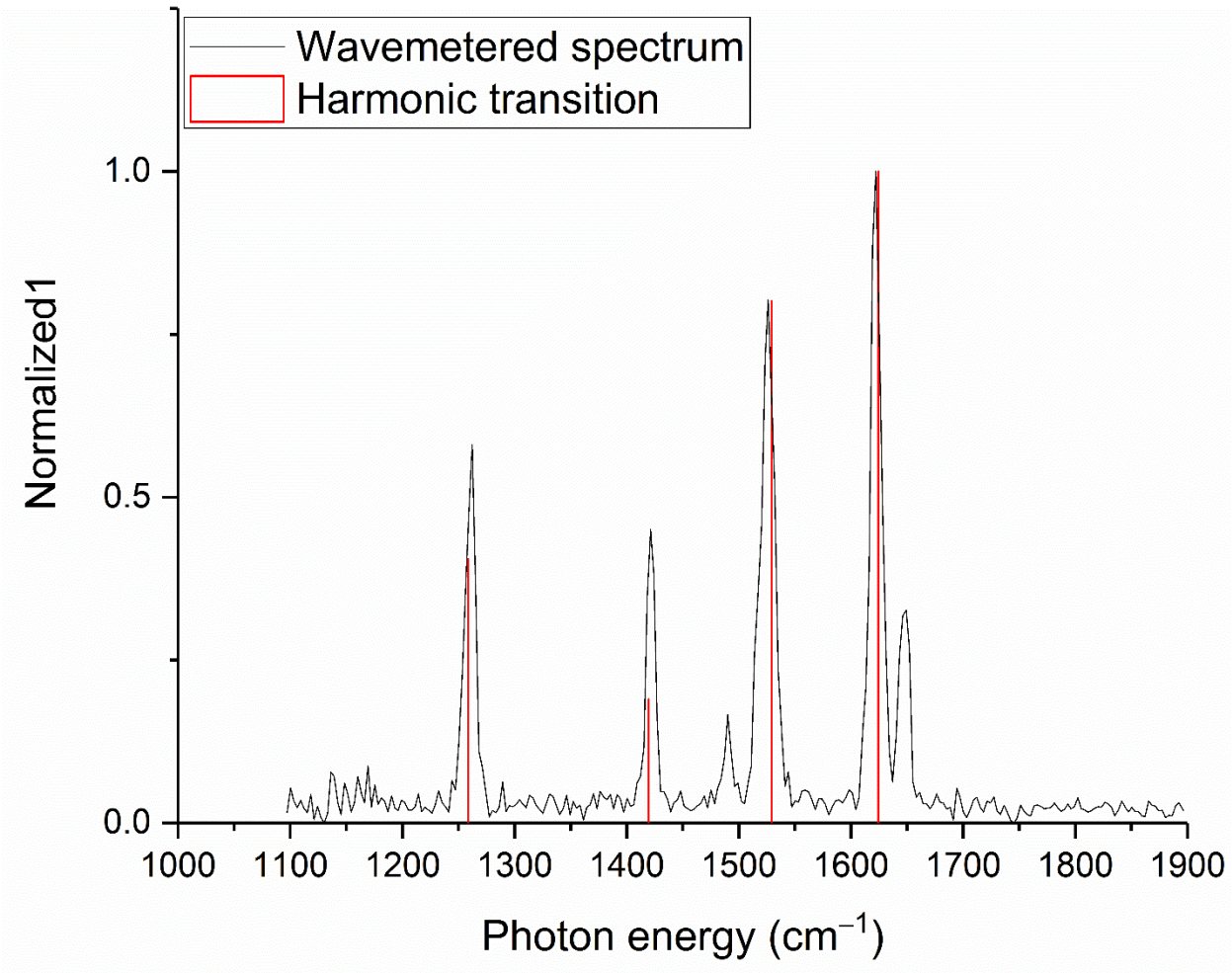

Figure S34. Calculated [MP2/def2-TZVPPD] vs. observed IR-spectra for $CsOx^-$.

Table S10. Calculated [MP2/def2-TZVPPD] and observed transitions for $CsOx^-$.

Description	Normal mode	Calculated transition (cm^{-1})	Scaled (×0.985) transition (cm^{-1})	Observed transition (cm^{-1})
Out-of-phase bound C=O and symmetric CO_2 stretch	ν_{12}	1278.03	1258.86	1257.94
In-phase bound C=O and symmetric CO_2 stretch	ν_{13}	1441.01	1419.40	1420.74
Antisymmetric CO_2 stretch	ν_{14}	1552.45	1529.16	1528.29
Unbound C=O stretch	ν_{15}	1649.14	1624.40	1625.78

SI-J. Cartesian coordinates for the MCO_2^- geometries optimized on the [CCSD(T)/def2-TZVPPD] level of theory

Lithium A isomer

C	0.00000000	0.00000000	-0.62166437
O	-1.12949325	0.00000000	-0.05993573
O	1.12949325	0.00000000	-0.05993573
Li	0.00000000	0.00000000	1.54016564

Lithium B isomer

C	-0.22916797	0.17526263	0.00000000
O	-0.12015001	1.38742865	0.00000000
O	0.59818564	-0.79518546	0.00000000
Li	-0.81697026	-1.91688324	0.00000000

Sodium A isomer

C	0.00000000	0.00000000	1.10447983
O	0.00000000	1.13664696	0.58893580
O	0.00000000	-1.13664696	0.58893580
Na	0.00000000	0.00000000	-1.44592518

Sodium B isomer

C	0.00000000	0.72189100	0.00000000
O	-0.18939800	1.92319000	0.00000000
O	0.96504500	-0.07450400	0.00000000
Na	-0.56410700	-1.73825700	0.00000000

Potassium A isomer

C	0.00000000	0.00000000	-1.55114100
O	0.00000000	1.14170200	-1.05253300
O	0.00000000	-1.14170200	-1.05253300
K	0.00000000	0.00000000	1.37617700

Potassium B isomer

C	0.10454624	-1.26957068	0.00000000
O	0.49883946	-2.42203076	0.00000000
O	-0.97608899	-0.64823564	0.00000000
K	0.18028146	1.68802389	0.00000000

Rubidium A isomer

C	0.00000000	0.00000000	2.07313321
O	0.00000000	1.14211461	1.58028214
O	0.00000000	-1.14211461	1.58028214
Rb	0.00000000	0.00000000	-0.99308527

Rubidium B isomer

C	0.10486370	-1.87607566	0.00000000
O	0.55761475	-3.00661055	0.00000000
O	-1.00061520	-1.30458889	0.00000000
Rb	0.08027922	1.20584642	0.00000000

Cesium A isomer

C	0.00164000	2.40405600	-0.00076400
O	1.14250300	1.90272700	0.00141700
O	-1.14023000	1.90507400	0.00141800
Cs	-0.00172400	-0.79794800	-0.00118600

Cesium B isomer

C	0.12137171	-2.25809424	0.00000000
O	0.54232712	-3.40141016	0.00000000
O	-0.97617654	-1.66635471	0.00000000
Cs	0.04115927	0.97001573	0.00000000

Carbon dioxide

C	0.00000000	0.00000000	0.00000000
O	0.00000000	0.00000000	-1.16594614
O	0.00000000	0.00000000	1.16594614

SI-K. Cartesian coordinates for [MP2/def2-TZVPPD] optimized species formed during MOx^- dissociation

The nomenclature for the structures reported in this section is equivalent to that used in section SI-E and Figure S21 to Figure S25.

Lithium

1A

Center Number	Atomic Number	Atomic Type	Coordinates (Angstroms) X	Y	Z
1	6	0	-2.913516	0.403028	-0.031874
2	6	0	-4.513180	0.409636	-0.031874
3	8	0	-2.315120	1.478354	-0.031874
4	8	0	-2.363210	-0.775792	-0.031874
5	8	0	-5.102672	1.489869	-0.031874
6	8	0	-5.073206	-0.764598	-0.031874
7	3	0	-3.722924	-1.911928	-0.031873

TS1AB

Center Number	Atomic Number	Atomic Type	Coordinates (Angstroms) X	Y	Z
1	6	0	-3.018513	0.303670	0.001620
2	6	0	-4.550213	0.316007	0.031460
3	8	0	-2.390083	1.216404	0.644954
4	8	0	-2.433512	-0.334683	-0.942924
5	8	0	-4.916118	1.193686	-0.815874
6	8	0	-5.219687	-0.424161	0.772786
7	3	0	-2.060248	1.499084	-1.192304

1B

Center Number	Atomic Number	Atomic Type	Coordinates (Angstroms) X	Y	Z
1	6	0	-3.036136	0.339363	-0.032358
2	6	0	-4.569781	0.375282	-0.030070
3	8	0	-2.374792	1.101320	0.766521
4	8	0	-2.413574	-0.452664	-0.833152
5	8	0	-5.073642	1.206038	-0.824883
6	8	0	-5.109610	-0.431029	0.766299
7	3	0	-0.948534	0.290469	-0.035472

2A

Center Number	Atomic Number	Atomic Type	Coordinates (Angstroms) X	Y	Z
1	6	0	-0.487526	1.028670	0.955446
2	8	0	0.704030	1.325256	0.738651
3	8	0	-1.559853	1.568233	0.618167
4	3	0	-0.229522	2.838036	-0.243532

TS2A

Center Number	Atomic Number	Atomic Type	Coordinates (Angstroms) X	Y	Z
1	6	0	-0.467241	1.028733	0.955030
2	8	0	0.530846	0.493903	1.290364
3	8	0	-1.230990	1.804392	0.456568
4	3	0	-0.405486	3.433167	-0.633230

INCAB

Center Number	Atomic Number	Atomic Type	Coordinates (Angstroms) X	Y	Z
1	6	0	-0.129154	-0.437278	0.290938
2	8	0	1.004247	-0.690963	0.438288
3	8	0	-1.275448	-0.229750	0.174285
4	3	0	0.789570	2.851852	-1.896513

TS1B

Center Number	Atomic Number	Atomic Type	Coordinates (Angstroms) X	Y	Z
1	6	0	-1.640336	0.295600	0.102543
2	6	0	-4.608578	0.290276	-0.161056
3	8	0	-1.472439	1.330849	-0.416351
4	8	0	-1.664947	-0.731343	0.677554
5	8	0	-4.938003	1.454514	-0.127763
6	8	0	-4.974621	-0.787279	0.406295
7	3	0	-3.896093	-1.702683	-0.704337

INC1B

Center Number	Atomic Number	Atomic Type	Coordinates (Angstroms) X	Y	Z
1	6	0	-1.425993	0.698642	0.220128
2	6	0	-4.512886	-0.132798	-0.058198
3	8	0	-1.429187	1.217086	-0.827947
4	8	0	-1.343643	0.196235	1.272773
5	8	0	-4.169717	0.921440	0.440132
6	8	0	-5.631681	-0.698840	-0.287704
7	3	0	-4.685610	-2.053230	-0.984398

2B

Center Number	Atomic Number	Atomic Type	Coordinates (Angstroms) X	Y	Z
1	6	0	-0.595109	0.943437	0.520284
2	8	0	0.264499	1.004550	1.374773
3	8	0	-1.696449	1.549757	0.294234
4	3	0	-1.860841	0.517723	-1.163922

TS2AB

Center Number	Atomic Number	Atomic Type	Coordinates (Angstroms) X	Y	Z
1	6	0	-0.282073	0.933572	0.709019
2	8	0	0.734269	0.769646	1.366935
3	8	0	-1.128714	1.875727	0.600340
4	3	0	-0.896354	3.181249	-0.607562

TS2B

Center Number	Atomic Number	Atomic Type	Coordinates (Angstroms) X	Y	Z
1	6	0	-0.593271	1.157204	0.793201
2	8	0	0.375647	0.959831	1.418487
3	8	0	-1.610995	1.472137	0.272976
4	3	0	-2.059281	0.426294	-1.459293

Sodium

1A

Center Number	Atomic Number	Atomic Type	Coordinates (Angstroms) X	Y	Z
1	6	0	-2.926594	0.435793	-0.103358
2	6	0	-4.497768	0.452100	0.007287
3	8	0	-2.360228	1.397091	-0.639375
4	8	0	-2.341514	-0.616460	0.380437
5	8	0	-5.050694	1.470511	0.442360
6	8	0	-5.097377	-0.635883	-0.367380
7	11	0	-3.729989	-2.179325	0.085724

TS1AB

Center Number	Atomic Number	Atomic Type	Coordinates (Angstroms) X	Y	Z
1	6	0	-3.167487	0.432222	-0.115388
2	6	0	-4.686703	0.287978	0.050149
3	8	0	-2.564079	1.345703	0.548325
4	8	0	-2.589244	-0.223923	-1.050360
5	8	0	-5.292496	1.087250	-0.725059
6	8	0	-5.141553	-0.539168	0.869419
7	11	0	-1.770451	1.749223	-1.430441

1B

Center Number	Atomic Number	Atomic Type	Coordinates (Angstroms) X	Y	Z
1	6	0	-3.076309	0.341085	-0.031494
2	6	0	-4.614724	0.372893	-0.033545
3	8	0	-2.443725	1.111067	0.774991
4	8	0	-2.473946	-0.454431	-0.836334
5	8	0	-5.124787	1.201488	-0.829008
6	8	0	-5.160718	-0.433868	0.760512
7	11	0	-0.631861	0.290544	-0.028237

TS1A

Center Number	Atomic Number	Atomic Type	Coordinates (Angstroms) X	Y	Z
1	6	0	-2.834763	0.336068	-0.031178
2	6	0	-5.014469	0.381229	-0.034059
3	8	0	-2.348918	0.290378	1.106157
4	8	0	-2.344439	0.361533	-1.167223
5	8	0	-5.313381	0.423763	-1.194065
6	8	0	-5.317950	0.351177	1.125151
7	11	0	-0.352151	0.284631	-0.027897

INC1A

Center Number	Atomic Number	Atomic Type	Coordinates (Angstroms) X	Y	Z
1	6	0	-2.646852	0.332173	-0.030928
2	6	0	-5.446729	0.390181	-0.034636
3	8	0	-2.156383	1.119544	0.792129
4	8	0	-2.187236	-0.474881	-0.852726
5	8	0	-5.486471	1.231066	-0.848993
6	8	0	-5.523421	-0.448291	0.779566
7	11	0	-0.079580	0.278986	-0.027526

2A

Center Number	Atomic Number	Atomic Type	Coordinates (Angstroms) X	Y	Z
1	6	0	-0.486115	0.959057	1.009797
2	8	0	0.703206	1.267713	0.801795
3	8	0	-1.571719	1.466528	0.667812
4	11	0	-0.218244	3.066894	-0.410671

TS2A

Center Number	Atomic Number	Atomic Type	Coordinates (Angstroms) X	Y	Z
1	6	0	-0.435706	0.981976	0.994339
2	8	0	0.741732	0.837699	1.091859
3	8	0	-1.455741	1.504846	0.641726
4	11	0	-0.423157	3.435671	-0.659191

INCAB

Center Number	Atomic Number	Atomic Type	Coordinates (Angstroms) X	Y	Z
1	6	0	-0.066758	-1.185066	0.798593
2	8	0	1.100718	-1.253699	0.845135
3	8	0	-1.236680	-1.156943	0.779351
4	11	0	0.146330	2.345232	-1.580403

2B

Center Number	Atomic Number	Atomic Type	Coordinates (Angstroms) X	Y	Z
1	6	0	0.081715	-0.688035	0.000000
2	8	0	0.496386	-1.835928	-0.000000
3	8	0	-1.020467	-0.086226	-0.000000
4	11	0	0.350644	1.731656	-0.000000

TS2B

Center Number	Atomic Number	Atomic Type	Coordinates (Angstroms) X	Y	Z
1	6	0	-0.503999	-0.476056	0.002649
2	8	0	0.694486	-0.851011	-0.002052
3	8	0	-1.617842	-0.974998	0.007917
4	11	0	1.049959	1.398073	-0.005949

TS2AB

Center Number	Atomic Number	Atomic Type	Coordinates (Angstroms) X	Y	Z
1	6	0	-0.314403	1.008034	0.652266
2	8	0	0.709968	0.866770	1.314753
3	8	0	-1.378446	1.674150	0.752164
4	11	0	-0.589990	3.211238	-0.650449

Potassium

1A

Center Number	Atomic Number	Atomic Type	Coordinates (Angstroms) X	Y	Z
1	6	0	-2.937092	0.500535	-0.009708
2	6	0	-4.495008	0.495148	-0.071514
3	8	0	-2.355978	1.422288	0.586701
4	8	0	-2.374587	-0.514255	-0.582699
5	8	0	-5.081008	1.390001	-0.703076
6	8	0	-5.052107	-0.499726	0.540365
7	19	0	-3.708067	-2.469831	0.016815

TS1AB

Center Number	Atomic Number	Atomic Type	Coordinates (Angstroms) X	Y	Z
1	6	0	-2.989603	0.540985	-0.044171
2	6	0	-4.536146	0.672197	0.014496
3	8	0	-2.278399	1.160038	0.762738
4	8	0	-2.586689	-0.251509	-0.984123
5	8	0	-5.072298	1.688186	-0.479875
6	8	0	-5.154718	-0.364742	0.463315
7	19	0	-4.554595	-1.618663	-1.592475

1B

Center Number	Atomic Number	Atomic Type	Coordinates (Angstroms) X	Y	Z
1	6	0	-3.039535	-0.151920	0.452911
2	6	0	-4.374600	0.406195	-0.094189
3	8	0	-2.483219	0.504529	1.387554
4	8	0	-2.475327	-1.062417	-0.230194
5	8	0	-4.159556	1.320270	-0.978503
6	8	0	-5.471356	-0.015658	0.309059
7	19	0	-1.522476	1.427779	-1.069753

TS1A

Center Number	Atomic Number	Atomic Type	Coordinates (Angstroms) X	Y	Z
1	6	0	-2.344751	0.439743	-0.055094
2	6	0	-4.475404	0.484399	0.062018
3	8	0	-2.006719	1.564570	-0.318501
4	8	0	-2.027181	-0.698824	0.172277
5	8	0	-4.938930	1.609901	-0.153842
6	8	0	-4.959100	-0.621250	0.329944
7	19	0	-7.303488	0.543673	0.217466

INC1A

Center Number	Atomic Number	Atomic Type	Coordinates (Angstroms) X	Y	Z
1	6	0	2.772944	-0.058118	-0.152417
2	6	0	0.052071	-0.001092	-0.002862
3	8	0	2.802073	0.587120	-1.130416
4	8	0	2.882061	-0.706253	0.817984
5	8	0	-0.361068	0.967017	0.656728
6	8	0	-0.470919	-0.949580	-0.610998
7	19	0	-2.870549	0.060163	0.157781

2A

Center Number	Atomic Number	Atomic Type	Coordinates (Angstroms) X	Y	Z
1	6	0	-0.486452	1.242447	-0.488211
2	8	0	0.666485	1.234348	-0.006517
3	8	0	-1.629261	1.233867	0.017036
4	19	0	-0.456488	1.193109	2.431398

TS3A

Center Number	Atomic Number	Atomic Type	Coordinates (Angstroms) X	Y	Z
1	6	0	-0.486317	1.240415	-0.409047
2	8	0	0.686382	1.235780	-0.179900
3	8	0	-1.653681	1.237244	-0.154096
4	19	0	-0.452099	1.190332	2.696748

INCAB

Center Number	Atomic Number	Atomic Type	Coordinates (Angstroms) X	Y	Z
1	6	0	-0.023617	0.034568	-2.143644
2	8	0	1.146176	0.034121	-2.174239
3	8	0	-1.193800	0.035585	-2.148435
4	19	0	0.029368	-0.042985	2.665626

TS2A

Center Number	Atomic Number	Atomic Type	Coordinates (Angstroms) X	Y	Z
1	6	0	-2.912510	-0.294876	0.594856
2	6	0	-4.797871	0.598683	-0.284507
3	8	0	-2.486431	0.529823	1.395312
4	8	0	-2.477015	-1.069179	-0.249656
5	8	0	-4.232441	1.378197	-1.039066
6	8	0	-5.842538	0.178498	0.118035
7	19	0	-1.614169	1.432071	-1.076422

INC2A

Center Number	Atomic Number	Atomic Type	Coordinates (Angstroms) X	Y	Z
1	6	0	0.375976	-1.052663	1.114643
2	6	0	-2.010621	0.129509	-0.188209
3	8	0	0.754132	0.006231	1.647807
4	8	0	0.503461	-1.558539	-0.017013
5	8	0	-1.354175	0.894577	-0.784961
6	8	0	-2.706344	-0.609096	0.391819
7	19	0	1.688385	0.772365	-0.801779

2B

Center Number	Atomic Number	Atomic Type	Coordinates (Angstroms) X	Y	Z
1	6	0	0.081991	-1.214525	-0.000000
2	8	0	0.545537	-2.349656	0.000000
3	8	0	-1.049414	-0.671473	0.000000
4	19	0	0.229465	1.583840	0.000000

TS2B

Center Number	Atomic Number	Atomic Type	Coordinates (Angstroms) X	Y	Z
1	6	0	-0.020257	-1.353245	0.001104
2	8	0	0.593435	-2.374603	-0.000425
3	8	0	-1.013044	-0.668321	0.005341
4	19	0	0.247443	1.744356	-0.006020

TS2AB

Center Number	Atomic Number	Atomic Type	Coordinates (Angstroms) X	Y	Z
1	6	0	-0.356942	1.510654	-0.190608
2	8	0	0.707759	1.043349	-0.604937
3	8	0	-1.480378	1.046046	0.129924
4	19	0	-0.776155	1.303722	2.619327

Rubidium

1A

Center Number	Atomic Number	Atomic Type	Coordinates (Angstroms) X	Y	Z
1	6	0	-2.862757	0.558561	-0.260334
2	6	0	-4.395250	0.375034	-0.169524
3	8	0	-2.353809	1.592874	-0.722504
4	8	0	-2.254949	-0.483017	0.198243
5	8	0	-4.939918	0.642045	0.946429
6	8	0	-4.952472	-0.270937	-1.110554
7	37	0	-4.245007	-2.090733	0.923940

TS1A

Center Number	Atomic Number	Atomic Type	Coordinates (Angstroms) X	Y	Z
1	6	0	-2.459258	0.993948	-0.456723
2	6	0	-4.094376	-0.240256	0.102260
3	8	0	-2.733394	1.438202	-1.542336
4	8	0	-1.672470	0.936647	0.453633
5	8	0	-3.936490	-0.763012	1.210863
6	8	0	-4.982344	-0.268580	-0.756757
7	37	0	-6.374640	-1.961530	0.881766

INC1A

Center Number	Atomic Number	Atomic Type	Coordinates (Angstroms) X	Y	Z
1	6	0	2.755493	2.079942	-0.941977
2	6	0	0.679447	0.512885	-0.232269
3	8	0	2.790913	1.664109	-2.037532
4	8	0	2.833979	2.581755	0.114639
5	8	0	1.050929	-0.580647	0.226610
6	8	0	-0.416339	1.059691	-0.443540
7	37	0	-1.671605	-1.261756	0.571451

2A

Center Number	Atomic Number	Atomic Type	Coordinates (Angstroms) X	Y	Z
1	6	0	-0.000000	-0.000000	2.070993
2	8	0	0.000000	1.147492	1.573315
3	8	0	0.000000	-1.147492	1.573315
4	37	0	-0.000000	0.000000	-0.977010

TS3A

Center Number	Atomic Number	Atomic Type	Coordinates (Angstroms) X	Y	Z
1	6	0	0.000000	0.000000	1.979162
2	8	0	-0.000000	1.169644	1.729549
3	8	0	-0.000000	-1.169644	1.729549
4	37	0	0.000000	-0.000000	-1.197647

INCAB

Center Number	Atomic Number	Atomic Type	Coordinates (Angstroms) X	Y	Z
1	6	0	-0.000000	0.000000	2.924511
2	8	0	0.000000	1.170044	2.940626
3	8	0	0.000000	-1.170044	2.940626
4	37	0	0.000000	-0.000000	-1.994718

TS2A

Center Number	Atomic Number	Atomic Type	Coordinates (Angstroms) X	Y	Z
1	6	0	-2.523854	0.628253	-0.291761
2	6	0	-4.757001	0.397515	-0.178770
3	8	0	-2.106016	1.652330	-0.748360
4	8	0	-2.240608	-0.460620	0.190293
5	8	0	-5.072893	0.603203	0.986693
6	8	0	-5.082810	-0.327836	-1.110494
7	37	0	-4.220979	-2.169017	0.958095

INC2A

Center Number	Atomic Number	Atomic Type	Coordinates (Angstroms) X	Y	Z
1	6	0	1.782012	1.547272	-0.665927
2	6	0	-1.161376	1.362671	-0.660087
3	8	0	1.743390	2.653091	-1.041879
4	8	0	1.873674	0.439263	-0.296976
5	8	0	-0.976655	1.458066	0.569811
6	8	0	-1.227556	0.410528	-1.460389
7	37	0	-0.449433	-1.335661	0.646678

2B

Center Number	Atomic Number	Atomic Type	Coordinates (Angstroms) X	Y	Z
1	6	0	0.082164	-1.815632	0.000000
2	8	0	0.602822	-2.928218	-0.000000
3	8	0	-1.078740	-1.337813	-0.000000
4	37	0	0.135896	1.100234	-0.000000

TS2B

Center Number	Atomic Number	Atomic Type	Coordinates (Angstroms) X	Y	Z
1	6	0	-0.003457	-1.956323	-0.001177
2	8	0	0.642306	-2.960438	0.002503
3	8	0	-1.032163	-1.322724	-0.009430
4	37	0	0.135458	1.258056	0.008104

TS2AB

Center Number	Atomic Number	Atomic Type	Coordinates (Angstroms) X	Y	Z
1	6	0	0.272045	0.119899	1.747857
2	8	0	-0.198876	1.187960	2.155257
3	8	0	-0.186221	-1.020143	1.484280
4	37	0	0.113052	-0.287715	-1.146781

Cesium

1A

Center Number	Atomic Number	Atomic Type	Coordinates (Angstroms) X	Y	Z
1	6	0	-2.863666	0.581661	-0.265974
2	6	0	-4.392577	0.393441	-0.173796
3	8	0	-2.349487	1.616204	-0.718524
4	8	0	-2.262480	-0.467984	0.185482
5	8	0	-4.934034	0.644017	0.947409
6	8	0	-4.948185	-0.251665	-1.116240
7	55	0	-4.253735	-2.191845	0.947338

TS1A

Center Number	Atomic Number	Atomic Type	Coordinates (Angstroms) X	Y	Z
1	6	0	-2.458203	1.043363	-0.475196
2	6	0	-4.101864	-0.250428	0.105426
3	8	0	-2.764160	1.480966	-1.552117
4	8	0	-1.671937	0.983830	0.432057
5	8	0	-3.921947	-0.776813	1.208652
6	8	0	-4.997378	-0.287319	-0.745017
7	55	0	-6.438447	-2.089646	0.930821

INC1A

Center Number	Atomic Number	Atomic Type	Coordinates (Angstroms) X	Y	Z
1	6	0	3.134081	2.466960	-1.107111
2	6	0	1.078290	0.848765	-0.380905
3	8	0	3.157341	2.052687	-2.202922
4	8	0	3.207432	2.957280	-0.045427
5	8	0	1.473897	-0.240974	0.066870
6	8	0	-0.028571	1.378648	-0.577430
7	55	0	-1.330224	-1.047073	0.469900

2A

Center Number	Atomic Number	Atomic Type	Coordinates (Angstroms) X	Y	Z
1	6	0	-2.382375	0.000023	0.000207
2	8	0	-1.884071	-1.147556	0.000135
3	8	0	-1.884038	1.147588	0.000135
4	55	0	0.788498	-0.000023	-0.000248

TS3A

Center Number	Atomic Number	Atomic Type	Coordinates (Angstroms) X	Y	Z
1	6	0	-2.300623	0.000022	0.000195
2	8	0	-2.040143	-1.169538	0.000157
3	8	0	-2.040109	1.169574	0.000157
4	55	0	1.018888	-0.000026	-0.000282

INCAB (not converged)

Center Number	Atomic Number	Atomic Type	Coordinates (Angstroms) X	Y	Z
1	6	0	-3.235214	0.000047	0.000464
2	8	0	-3.246891	-1.170962	0.000466
3	8	0	-3.246857	1.171056	0.000466
4	55	0	1.073625	-0.000016	-0.000154

TS2A

Center Number	Atomic Number	Atomic Type	Coordinates (Angstroms) X	Y	Z
1	6	0	-2.158527	0.761492	-0.353733
2	6	0	-4.414574	0.484196	-0.209810
3	8	0	-1.767357	1.796397	-0.808050
4	8	0	-1.857740	-0.326466	0.116529
5	8	0	-4.710348	0.677567	0.961369
6	8	0	-4.732070	-0.238602	-1.144312
7	55	0	-3.803465	-2.210392	0.956286

INC2A

Center Number	Atomic Number	Atomic Type	Coordinates (Angstroms) X	Y	Z
1	6	0	1.822962	2.005103	-0.847653
2	6	0	-1.078955	1.678492	-0.816626
3	8	0	1.751722	3.129239	-1.159410
4	8	0	1.949391	0.880341	-0.545817
5	8	0	-0.891326	1.793911	0.411061
6	8	0	-1.237533	0.716788	-1.590941
7	55	0	-0.382207	-1.112981	0.574040

2B

Center Number	Atomic Number	Atomic Type	Coordinates (Angstroms) X	Y	Z
1	6	0	0.091493	-2.193041	0.000000
2	8	0	0.597483	-3.310963	-0.000000
3	8	0	-1.062710	-1.697859	-0.000000
4	55	0	0.102417	0.846020	-0.000000

TS2B

Center Number	Atomic Number	Atomic Type	Coordinates (Angstroms) X	Y	Z
1	6	0	0.012376	-2.352642	0.000265
2	8	0	0.617137	-3.380621	0.000323
3	8	0	-0.983810	-1.670951	0.000584
4	55	0	0.082980	1.048372	-0.001171

TS2AB

Center Number	Atomic Number	Atomic Type	Coordinates (Angstroms) X	Y	Z
1	6	0	-2.064700	-0.115780	-0.278036
2	8	0	-2.465967	-1.184099	0.198318
3	8	0	-1.780059	1.018185	0.187371
4	55	0	0.948740	0.281726	-0.107423

Carbon dioxide

Center Number	Atomic Number	Atomic Type	Coordinates (Angstroms) X	Y	Z
1	6	0	0.345953	2.167102	0.000000
2	8	0	-0.823110	2.167102	0.000000
3	8	0	1.515016	2.167102	0.000000

References

(1) Fairley, D. A.; Scott, G. B. I.; Freeman, C. G.; Maclagan, R. G. A. R.; McEwan, M. J. C $_2$ H $_7$ O $^+$ Potential Surface and Ion−Molecule Association between H_3O^+ and C_2H_4. *J. Phys. Chem. A* **1997**, *101* (15), 2848–2851. https://doi.org/10.1021/jp963294c.

(2) Dawson, P. H. A Study of the Collision-Induced Dissociation of $C_2H_5OH_2^+$ Using Various Target Gases. *Int. J. Mass Spectrom. Ion Phys.* **1983**, *50* (3), 287–297. https://doi.org/10.1016/0020-7381(83)87006-5.

(3) Bouchoux, G.; Hoppilliard, Y. Role of Ion-Neutral Complexes during Acid-Catalyzed Dehydration of Ethanol in the Gas Phase. *J. Am. Chem. Soc.* **1990**, *112* (25), 9110–9115. https://doi.org/10.1021/ja00181a012.

(4) Graul, S. T.; Squires, R. R. Gas-Phase Acidities Derived from Threshold Energies for Activated Reactions. *J. Am. Chem. Soc.* **1990**, *112* (7), 2517–2529. https://doi.org/10.1021/ja00163a007.

(5) Skripnikov, L. V. *Chemissian Version 4.52, Visualization Computer Program*; 2017.

(6) Xantheas, S. S. On the Importance of the Fragment Relaxation Energy Terms in the Estimation of the Basis Set Superposition Error Correction to the Intermolecular Interaction Energy. *J. Chem. Phys.* **1996**, *104* (21), 8821–8824. https://doi.org/10.1063/1.471605.